

Cell-lineage specificity of primary cilia during epididymis post-natal development

Agathe Bernet¹, Alexandre Bastien², Denis Soulet³, Olivia Jerczynski¹, Christian Roy¹, Maira Bianchi Rodrigues Alves¹, Cynthia Lecours^{3,4}, Marie-Ève Tremblay⁴, Janice Bailey², Claude Robert², Clémence Belleannée^{1,5}.

¹ Department of Obstetrics, Gynecology and Reproduction, Université Laval, CHU de Québec Research Center (CHUL), Quebec City, Quebec, Canada.

² Department of Animal Sciences, Université Laval, Quebec City, Quebec, Canada.

³ Faculty of Pharmacy, Université Laval, CHU de Québec Research Center (CHUL), Quebec City, Quebec, Canada.

⁴ Department of Molecular Medicine, Université Laval, CHU de Québec Research Center (CHUL), Quebec City, Quebec, Canada.

⁵ *Corresponding author*

E-mail to CB: Clemence.Belleannee@crchudequebec.ulaval.ca

30 **Abstract**

31 Primary cilia are sensory organelles that orchestrate major signaling pathways during organ
32 development and homeostasis. By using a double Arl13b/mCherry-Cetn2/GFP transgenic mouse
33 model, we characterized the spatio-temporal localization of primary cilia in the epididymis, from
34 birth to adulthood. We report here a constitutive localisation of primary cilia in peritubular
35 myoid cells and a dynamic profiling in differentiated epithelial cells throughout post-natal
36 development. While primary cilia are present at the apical pole of the undifferentiated epithelial
37 cells from birth to puberty, they are absent from the apical pole of the epithelium in adults,
38 where they appear exclusively associated with cytokeratin 5-positive basal cells. Exogenous
39 labeling of primary cilia marker Arl13b and IFT88 confirmed the cell lineage specific localization
40 of primary cilia in basal cells and myoid cells in human epididymides. From whole epididymis
41 tissues and serum-free cultures of DC2 murine epididymal principal cell lines we determined
42 that primary cilia from the epididymis are associated with the polycystic kidney disease-related
43 proteins polycystin 1 (PC1) and polycystin 2 (PC2), and Gli3 Hedgehog signaling transcription
44 factor. Thus, our findings unveil the existence of primary cilia sensory organelles, which have the
45 potential to mediate mechano/ chemo-signaling events in the epididymis.

46 **Introduction**

47 Post-natal development (PND) of the epididymis is a multistep process synchronized
48 with an increase in androgen plasma level, arrival of testicular flow, and sperm release [1].
49 Proper epididymis PND is essential to generate a fully functional organ that will ensure optimal
50 post-testicular sperm maturation at the time of puberty (For review, [2]). Thus, identification of
51 cellular factors involved in the development of male reproductive functions is a compelling
52 research avenue that may help understand the aetiology of some unexplained male infertility
53 issues.

54 The adult epididymis is a single convoluted tubule divided into three to four main
55 anatomical regions (*i.e.* initial segment in rodents, *caput*, *corpus* and *cauda*), each displaying
56 distinct morphological features. The lumen of the epididymis through which spermatozoa
57 transit is surrounded by a pseudostratified epithelium. The latter is mainly composed of
58 principal, clear and basal cells, whose functions are essential to ensure proper post-testicular
59 sperm maturation (for review [3]). The epididymis becomes fully functional following a series of
60 morphological changes that occur during its PND, particularly prior to puberty. These changes
61 include the formation and maintenance of a blood-epididymis barrier, the differentiation and
62 organization of epididymal cells to form a well-orchestrated pseudo-stratified epithelium, and
63 the regionalized expression of epididymal genes in the different segments of the organ.

64 The differentiation of epididymal cell populations and the establishment of distinct
65 epididymal segments was studied in different species during the 80's, including in mice, rats and
66 humans [1, 4-11]. It consists of three main stages: the undifferentiated period, the period of
67 differentiation, and the period of expansion [12]. During the undifferentiated period (1st week in
68 mouse), the epididymis epithelium is characterized by the presence of columnar cells that lack
69 stereocilia and form primitive junctions. The period of differentiation (2nd to 5th week in mouse)
70 consists in the appearance of differentiated and specialized cells, including clear, principal and
71 basal cells [13, 14] ; this period is associated with high cellular proliferation within the initial
72 segment. It has been proposed that the flow of testicular-derived fluid entering the epididymis
73 before sperm production may stimulate this proliferation/differentiation stage [1]. Finally, the
74 period of expansion (6th to 8th week in mouse) features the appearance of spermatozoa within

75 the epididymal lumen, as well as an increase in the size of the epididymis, until cell division
76 arrest at around the 10th week. Different factors such as luminal flow, lumicrine components
77 and androgens have been shown to participate in epididymis PND through epithelial cell
78 differentiation [15], [7, 16]; For review refer to [17]. However, the cellular mechanisms involved
79 in this process are unknown. The serendipitous finding of the presence of sensory primary cilia
80 organelles in the mammalian epididymis shed light on new potential developmental
81 mechanisms [18].

82 The primary cilium is a solitary cell extension that serves as a sensory organelle and a
83 signaling hub to control cell proliferation, migration, differentiation and planar polarity [19, 20].
84 Thus, this biological antenna is required to ensure proper tissue development and homeostasis
85 and extends from the surface of most mammalian cells at the post-mitotic stage. Non-motile
86 primary cilia are composed of a 9+0 axoneme (nine pairs of microtubules without central pair, in
87 contrast to 9+2 motile cilia) and a basal body, which derives from the mother centriole of the
88 centrosome. Depending on the biological system in which they are studied, primary cilia play
89 two distinct roles: one as a signaling mediator through a variety of ciliary receptors and their
90 downstream effector molecules, and the other as a mechanosensor through ion channels and
91 transporter proteins. The signaling pathways coordinated by primary cilia are diverse and
92 include Hedgehog (Hh)[21], Wingless (Wnt/Notch) [22] and Platelet-derived growth factor
93 receptor (PDGFR) [23] signaling pathways. In addition to this function, some cells are responsive
94 to the shear stress exerted by the surrounding biological fluids through primary cilia
95 mechanosensing [24], for review [25]. For instance, primary cilia found at the surface of renal
96 intercalated cells, sense urine flow and control cell proliferation through ciliary Polycystin 1
97 (PC1), transient receptor potential channel interacting, and the Polycystin 2 (PC2) cation
98 channel[26]. Bending of the primary cilium triggered by flow within the nephron tubule induces
99 calcium influx via PC2 calcium transporter, and the downstream regulation of target gene
100 expression involved in cell proliferation [26].

101 Based on remarkable studies asserting the role of primary cilia in cell sensing, the
102 functional features associated with this organelle make it an ideal candidate for detecting and
103 transducing signals involved in organ development. Apart from the serendipitous observation of

104 primary cilia in the epididymis of equine species reported by Arrighi in 2013 [18], no further
105 studies have investigated the characterization and potential role of these biological antennae in
106 epididymis development and homeostasis. In our study, we discovered for the first time the
107 presence of a primary cilia component in the human epididymis and portrayed their spatio-
108 temporal localization during epididymis PND in a double transgenic mouse model *Arl13b-*
109 *mCherry/Centrin2-GFP* [27]. Of relevance, impairment of primary cilia function is associated
110 with male infertility issues and other human diseases referred to as ciliopathies [28]. For
111 instance several reports indicate that Autosomal Polycystic Kidney Disease (APKD), a ciliopathy
112 affecting one in 800-1000 live birth, is associated with a higher prevalence of obstructive
113 azoospermia, increased epididymis and *vas deferens* volumes, and the presence of cysts in the
114 epididymis, seminal vesicles and prostate [29-31]. In addition, Von Hippel-Lindau Syndrome
115 (VHL), an autosomal dominant ciliopathy characterized by the predisposition for multiple
116 tumours, is associated with the development of epididymal cystadenomas that result in male
117 infertility when bilateral [32-35]. Considering that non-genetic environmental insults, such as
118 lithium treatment and folic acid uptake, have been shown to alter cilia length and functions [36-
119 40], portraying and unravelling the role of primary cilia during epididymis PND will open new
120 avenues concerning the diagnosis of unexplained male infertility cases.

121 **Material and Methods**

122 **Human tissues and ethical consent**

123 Human epididymides were obtained from donors between 26 and 50 years of age through our
124 local organ transplantation program (Transplant Quebec, QC, Canada) after obtaining written
125 consent from the families. Experiments performed in our study were in compliance with the
126 Declaration of Helsinki and were conducted according to the policies for Human Studies with
127 ethical approval from the Centre Hospitalier Universitaire's (CHUQ) Institutional Review Board
128 (#2018-4043). Human epididymides from three donors were processed as previously described
129 (ref [41]). In brief, the testicles were removed under artificial circulation to preserve tissues
130 assigned for transplantation and processed within 6 h. The epididymides were dissected into
131 three segments, *i.e.* caput, corpus and cauda and fixed by immersion in paraformaldehyde 4%
132 for immunohistological localization of Arl13b and IFT88.

133

134 **Mouse tissues and ethics**

135 Epididymides from C57BL/6 and Tg(CAG-Arl13b/mCherry)1Kvand Tg(CAG-EGFP/CETN2)3-
136 4Jgg/KvandJ (referred to as Arl13b-Cetn2 tg in this study, Jackson Laboratory stock# #027967)
137 were used in this study. The Arl13b-Cetn2 tg double transgenic mice express both the ciliary
138 component ADP-ribosylation factor-like protein 13B (Arl13b) fused to the monomeric red
139 fluorescence protein mCherry and the centriolar protein Centrin2 (Cetn2) fused to GFP [27].
140 These mice were housed and reproduced in the elite animal facility of the CHU de Quebec
141 research Center. Animal experiments were approved by the ethical committee of the
142 Institutional Review Board of the Centre Hospitalier Universitaire de Québec (CHUQ)(CPAC
143 licenses 2016050 and 12016051, C. Belleannée) and were conducted in accordance with the
144 requirements defined by the Guide for the Care and Use of Laboratory Animals.

145 Epididymides were obtained from mice sacrificed at different post-natal ages. Post-natal day 1
146 (1 dpn) to 268 dpn tissues were either 1) directly snap frozen in liquid nitrogen and stored at
147 -80°C until use, 2) fixed with fixative containing 4% paraformaldehyde, 10 mM sodium
148 periodate, 75 mM lysine, and 5% sucrose in 0.1 M sodium phosphate buffer (PLP) by immersion
149 (1 to 28 dpn) or by perfusion via the left ventricle (28 to 56 dpn) as previously described [42], or

150 3) fixed by intra-cardiac systemic fixation with 4% paraformaldehyde for transmission electron
151 microscopy (TEM) analysis as previously described and adapted [43].

152
153 **Cell culture**
154 Immortalized Distal Caput principal cells (DC2) developed from mouse tissues were kindly
155 provided by Marie-Claire Orgebin-Crist [44]. DC2 cell were maintained in Iscove's Modified
156 Dulbecco's Media (IMDM, Gibco, Invitrogen S.A.) containing 1 μ M dihydrotestosterone (Fluka),
157 10 % of fetal bovine serum (FBS) (Gibco, Invitrogen S.A.) and 50 U ml⁻¹ of penicillin G and
158 50 μ g ml⁻¹ streptomycin (Gibco, Invitrogen S.A.). Cells were kept in an incubator at 32,8 °C in 5%
159 CO₂ in air and 100% humidity. On the day before the experiment, DC2 cells were plated on
160 fibronectin treated coverslips in a 6-well plate at a density of a 125 000 cells per well. Cells were
161 starved from serum overnight prior to being fixed and used for immunofluorescence staining.

162
163 **Immunofluorescence staining**
164 Epididymides from Arl13b-Cetn2 tg mice fixed with PLP were treated for immunofluorescence
165 as previously described [45]. In brief, after three washes in PBS, tissues were cryoprotected with
166 30% sucrose in PBS for several hours at 4°C, embedded in Tissue-Tek® O.C.T. Compound
167 (Sakura® Finetek, USA), and quick-frozen. Five to 25- μ m-thick sections were cut on a cryostat
168 (Shandon Cryotome, Thermo) and collected onto Superfrost/Plus slides (Superfrost
169 Fisherbrand™). For indirect immunofluorescence staining, sections were hydrated for 15 min in
170 PBS and treated for 4 min with 1% Sodium Dodecyl Sulfate (SDS) and 2% Triton X-100 in PBS.
171 Sections were washed in PBS for 5 min and then blocked in PBS containing 1% BSA for 15 min.
172 Sections were then incubated overnight in a humid chamber at 4°C with primary antibodies
173 diluted in DAKO solution (DAKO Corp., Carpinteria, CA) and directed against specific markers of
174 basal, principal, clear and myoid cells as well as primary cilia components (**Table 1**). When
175 specified, an antigen retrieval step for 10 min at 110°C in citrate buffer was included prior to
176 incubation with the primary antibodies. Sections were washed in high-salt PBS (2.7% NaCl) twice
177 for 5 min and once in normal PBS. Respective secondary antibodies were then applied for 1 h at
178 room temperature followed by washes, as described above. Characteristics of these antibodies

179 are described in **Table 1**. Slides were mounted in Vectashield medium containing 4',6' -
180 diamidino-2-phenylindole (DAPI; Vector Laboratories, Inc., Burlingame, CA) for imaging.
181 For Immunofluorescence assays performed on cells, the latter were plated on fibronectin
182 coated slides at a density of 125 000 cells per well and fixed with 4% PFA for 10 min. After
183 washes with PBS, blocking was performed for 30 min in PBS solution with 1% BSA and 0.1%
184 Triton X-100. Slides were incubated for 1 hr. with primary antibody (1:400) followed by washes,
185 and for 1 hour with the appropriate secondary antibody (1:800). Slides were mounted in
186 Vectashield medium, as described above.

187
188 **Confocal imaging**
189 Digital images were acquired by confocal microscopy on an inverted Olympus IX80 microscope
190 equipped with a WaveFX-Borealin-SC Yokagawa spinning disk (Quorum Technologies; CFI
191 equipment to SE) and an Orca Flash4.0 camera (Hamamatsu). Image acquisition was performed
192 using Metamorph software (Molecular Devices). Optical Z-sections were acquired for each
193 channel and projected into a single picture using ImageJ. Low (20×) and high (100×)
194 magnification pictures were taken for the three major epididymis segments, the *caput*, *corpus*
195 and *cauda* epididymis.

196 Three-dimensional animations were generated with Bitplane Imaris software v7.5 (Bitplane,
197 Zurich, Switzerland) using images acquired by an Olympus FV-1000 confocal microscope
198 (Olympus Canada; CFI equipment to DS) equipped with a PLAPON60XOSC objective lens (NA
199 1.4). Isosurfaces were generated in the surpass module, and the camera was rotated to show
200 structures of interest. Generated isosurface renderings were rotated, panned, and zoomed
201 while recording the animation.

202 To determine primary cilia features throughout the epididymis, images were acquired on a Zeiss
203 LSM700 confocal microscope with a 40x/0.95 plan-apo lens. The resolution was set to the
204 highest possible according to the lens in use (0.145 $\mu\text{m}/\text{pixel}$). Whole epididymal sections (25
205 μm of thickness) were imaged in the z-axis, generally 15-20 μm at 1 μm interval and large
206 regions of at least 1 mm^2 were imaged in the XY plane with mosaic tiling at 10% overlap.
207 Excitation was done with lasers at 405, 488 and 555 nm while emission was selected with a

208 variable dichroic splitter. Large data processing was done with custom ImageJ [46] macro and
209 Matlab code. Briefly, images were converted from a single CZI mosaic file to multiple TIFFs. Each
210 tile was then compressed along the z-axis using a maximum intensity projection. Tiles were then
211 stitched together using MIST [47]. Gaussian filtering, thresholding and skeletonizing were
212 performed on the eGFP channel to outline distinct tubules. Centrosomes and cilia were
213 detected using ImageJ's Find Maxima. The centrosome list was filtered in Matlab to keep only
214 the closest to each cilium and cilia without visible centrosome were excluded. We determined
215 the absolute angle of each cilium with a rotating pattern in order to obtain a maximum at the
216 cilium angle relatively to the closest tubule edge. Matlab and ImageJ macro to process cilia
217 orientation from epididymal confocal acquisitions are available on
218 <https://github.com/alexandrebastien/Cilia>.

219
220 **Immunohistochemistry (IHC)**
221 Fixed epididymides from C57BL/6 mice were treated for IHC as previously described [48]. In
222 brief, tissues were dehydrated, embedded in paraffin and stored at 4°C until use. Paraffin
223 sections (5 µm thickness) were deparaffinised in toluene, hydrated, and then, where specified,
224 treated for antigen retrieval with citrate buffer (pH 6.0). Endogenous peroxidase activity was
225 then quenched with 3% H₂O₂ (v/v) in methanol for 10 min. Sections were washed for 5 min in
226 95% ethanol and 5 min in PBS. Non-specific binding sites were blocked with 0.5% BSA for 1 h.
227 Primary antibodies diluted in DAKO were applied overnight at 4°C (**Table 1**). For control
228 sections, PBS replaced the primary antibodies. Sections were subsequently incubated with
229 biotinylated 1) donkey anti-goat or 2) goat anti-rabbit antibodies for 60 min, and with ABC elite
230 reagent (Vector Laboratories, Inc. Burlingame, Ca) for 30 min. Immunostaining was revealed
231 using 3-amino-9-ethylcarbazole (AEC). Mayer's hematoxylin solution was used for
232 counterstaining, and mounted under cover slips using an aqueous mounting medium (Sigma).
233 Slides were observed under a Zeiss Axioskop 2 Plus microscope linked to a digital camera from
234 Qimaging. Images were captured using the QCapture Pro (Qimaging Instruments).

235
236 **Transmission Electron microscopy**

237 ***Tissue Preparation***

238 Mice were anesthetized with ketamine (intraperitoneally) and tissues were fixed by intracardiac
239 perfusion with PBS for 2 min followed by 4% PFA for 2 min and treated as previously described
240 and adapted [43]. In brief, tissues were further fixed by immersion for 2 h in 3.5% acrolein,
241 followed by 3 h in 4% PFA and washed three times in PBS for 15 min. Fifty-micrometer-thick
242 transverse sections of the epididymis were cut in PBS using a vibratome (Leica VT100S) and
243 stored at -20°C in cryoprotectant until further processing.

244

245 ***Electron microscopy***

246 Sections stored in cryoprotectant were rinsed in PBS, postfixed in 1% osmium tetroxide for 30
247 min at room temperature and dehydrated in ascending concentrations of ethanol (from 35% to
248 100%). Sections were then treated with propylene oxide and impregnated in Durcupan resin
249 (EMS) overnight at room temperature. After mounting between ACLAR embedding films (EMS),
250 the resin was polymerized at 55°C for 72 h. Areas of interest were excised from the embedding
251 films, re-embedded at the tip of resin blocks, and cut at 65–80 nm of thickness using an
252 ultramicrotome (Leica Ultracut UC7). Ultrathin sections were collected on square mesh grids
253 (EMS) and examined at 80 kV with an FEI Tecnai Spirit G2 transmission electron microscope.
254 Pictures were acquired using an Orca-HR camera (10 MP; Hamamatsu).

255

256

257 **Results**

258 **Primary cilia extend from basal and smooth muscle cells in the epididymis of adult mice**

259 Due to the fact that primary cilia are small, dynamic and present as a solitary figure on the cell
260 surface, these organelles are difficult to detect within *in situ* or *in vivo* whole organ systems. We
261 used the Arl13b-Cetn2 tg mouse model [27] to accurately study lineage specificity of primary
262 cilia from whole epididymis tissues. Arl13b-positive structures were observed within the
263 epithelium and in the surrounding smooth muscle layer of the epididymis (**Fig. 1A**). The
264 microtubule component and primary cilia marker acetylated tubulin (Ac-Tub) was observed
265 associated with the sperm flagellum and co-localized with Arl13b-positive cell extension, further
266 confirming the specific detection of non motile primary cilia from Arl13b-Cetn2 tg mice (**Fig.**
267 **1BC**). By using specific markers of distinct epididymis epithelial cell populations (*i.e.* keratin 5 for
268 basal cells, aquaporin 9 for principal cells and alpha actin for smooth muscle cells) we
269 determined the cell-specific localization of primary cilia from adult Arl13b-Cetn2 tg mice (**Fig. 2**).
270 As evidenced by labelling with the alpha actin smooth muscle cell marker, primary cilia were
271 found in the peritubular area associated with smooth muscle cell centriole (**Fig. 2A, inset**). The
272 ultrastructure of primary cilia in smooth muscle cells is composed of a basal centriole and an
273 axoneme extension as observed by transmission electron microscopy (**Fig. 2B**). In addition,
274 Arl13b-positive primary cilia were never observed associated with aquaporin 9-positive principal
275 cells, nor aquaporin 9-negative clear cells from adult mice (**Fig. 2C**). Finally, we found that
276 primary cilia extended from the centriole of keratin 5-positive basal cells (**Fig. 2D, inset**). From
277 the whole image acquisitions performed on adult epididymis tissues, all basal cells that were
278 observed within a 25 μ m tissue section exposed a primary cilium. While the major part of the
279 basal cell body is located at the base of the epithelium, basal cells dynamically extend towards
280 the lumen of the epididymis through axiopodia [49, 50]. According to basal cell 3D
281 reconstruction from transgenic epididymal tissues, we observed that primary cilia take their
282 origin from the centriole located at the apical pole of the cell body and at the base of the
283 axopodia (**Fig. 3**). In addition, basal cell-associated primary cilia never cross epididymis tight
284 junctions as evidenced by 3D reconstruction after ZO-1 staining (**Supplementary file 1**).

285

286 **Primary cilia profiling along the adult epididymis**

287 The epididymis is a highly segmented tubule with each segment displaying distinct features in
288 terms of cell populations, cell composition and cell functions [51]. We investigated the
289 properties of basal cell primary cilia throughout the different segments of the epididymis from
290 *Arl13b-Cetn2* tg mice (*i.e.* initial segment (IS), *caput*, *corpus* and *cauda*) by whole tissue confocal
291 imaging and digital image processing (**Fig. 4**). Primary cilia were observed associated with
292 peritubular myoid and basal cells in all segments of the epididymis, with a higher proportion in
293 the basal cells from the distal regions (**Fig. 4A, Supplementary file 2**). In the IS basal cell primary
294 cilia appeared as short 2–3 μm extensions directing towards the base of the epithelium,
295 according to GFP-positive centriole localization (**Figs. 4A, B**). In the other segments, *i.e.* the
296 *caput*, *corpus* and *cauda*, primary cilia appeared as longer 5–10 μm extensions, presenting with
297 erratic directions. Furthermore, myoid cell primary cilia presented no obvious variation from
298 one segment to another in terms of length (5–6 μm) or orientation (generally perpendicular to
299 the intratubular axis). In addition to their localization throughout the basal and peritubular
300 myoid cells of the epididymis, primary cilia were also associated with basal cells in the *vas*
301 *deferens* (VD) (**Fig. 4A, VD**) and were observed as tremendously long extensions in the *efferent*
302 *ducts* (ED) (**Fig. 4A, ED**). In ED, ciliated cells presenting with numerous *centrin2*-positive
303 centrioles were observed from the apical surface of the ducts. Moreover, elongated *Arl13b*-
304 positive primary cilia (15–40 μm) were found associated with centrioles located in non-ciliated
305 cells of the ED.

306

307 **Dynamic primary cilia exposure during epididymis post-natal development**

308 The epithelium of the epididymis undergoes important changes during the different PND stages
309 [1]. We explored the dynamics of primary cilia exposure that accompanies epididymis
310 epithelium development just after birth (at 5 dpn), at pre- and post-pubertal ages (at 30 and 42
311 dpn, respectively), and at the adult stage (at 42 to 268 dpn) (**Fig. 5**). The *Arl13b-Cetn2* tg mouse
312 model displays the same pattern of epididymis development as previously described in wild-
313 type mice [12] (**Fig. 5, Top**). For instance, H & E staining performed on the epididymis at 5 dpn
314 stage shows undifferentiated columnar cells of the epididymal epithelium surrounding an empty

315 lumen. At 30 dpn, we observed a pseudo-stratified epithelium and the presence of basal cells.
316 The lumen is filled with non-cellular material. At 42 dpn and 268 dpn, the pseudostratified
317 epithelium surrounds large lumens filled with spermatozoa. At an early stage of dpn (**Fig. 5, at 5**
318 **dpn Bottom and supplementary file 3**), primary cilia are observed by confocal microscopy as
319 short Arl13b-positive extensions associated with centrioles, located at the apical surface of non-
320 differentiated columnar cells. Primary cilia extensions are extensively observed associated with
321 myoid cells surrounding the epithelium. At 30 dpn, prior to puberty, primary cilia are found at
322 the apical surface of the epithelium associated with differentiated cells, potential clear and/or
323 principal cells, and associated with basal cells. After puberty, at 42 dpn (**Fig. 5, at 42 dpn and**
324 **supplementary file 4**) and 268 dpn, primary cilia extensions are exclusively found in basal cells
325 within the epithelium as well as in surrounding myoid cells. Thus, according to the PND stage of
326 the mouse epididymis, primary cilia are localized at different positions along the epididymal
327 epithelium, *i.e.* facing the lumen during the undifferentiated period, facing the lumen and at the
328 base of the epithelium during the period of differentiation, and exclusively at the base of the
329 epithelium during the expansion phase. Primary cilia are observed in myoid cells at all PND
330 stages studied. According to ZO-1 immunostaining of the apical pole of the epididymis (**Fig. 6**),
331 primary cilia extend from the epithelial cell surface at an early stage of PND (at 5 dpn) and are in
332 direct contact with the intraluminal compartment.

333 334 **Primary cilia of the epididymis are potential mechano/chemo-sensors of the cell-surrounding** 335 **environment**

336 According to the literature that describes the function of primary cilia in different model
337 systems, two major roles are associated with these biological antennae: the first as a chemo-
338 sensor of major signaling pathways (*e.g.* Hg, Wnt, PDGFR), and the second as a mechano-sensor
339 responsive to shear-stress and pressure exerted on the cell surface by extracellular bodily fluid.
340 By analogy with other tissues, we investigated the functional signaling components associated
341 with primary cilia in the epididymis.

342 We first explored the expression level of PC1 and PC2 (**Fig. 7**), two major players in the primary
343 cilia-dependent fluid-flow mechanosensation. At dpn 7, PC1 was detected at the apical pole of

344 undifferentiated cells as well as in peritubular myoid cells in the different epididymal segments
345 **(Fig. 7A)**. At this post-natal stage, a stronger signal was observed in the *vas deferens* **(Fig. 7A,**
346 **VD)**. In tissues from adult mice, PC1 was intensively detected in the cytoplasm and the apical
347 pole of the epithelium in the initial segment/*caput* of the epididymis. While PC1 intensity
348 transitionally decreased in the *corpus* compared to the *caput*, it drastically increased in the
349 apical membrane of epithelial cells from the *cauda* as well as in the *vas deferens* (VD). PC1 was
350 also detected, but to a lower extent, in the peritubular myoid cells. While PC2 could not be
351 detected on epididymal sections by IHC under our experimental conditions (not shown), we
352 observed a co-localisation between PC2 and the primary cilia marker Ac-Tub in the DC2
353 epididymal principal cell line **(Fig.7B, arrows)**.

354 We next investigated the expression of GLI3, a downstream transcriptional factor of the Hh
355 pathway **(Fig. 8)**. In adult epididymis, GLI3 was observed as discontinuous staining at the apical
356 pole of the epithelium in the *corpus* and *cauda* epididymidis. In addition, strong GLI3 staining
357 was observed in the nucleus of different epithelial cell populations in all segments of the organ.
358 This staining was particularly intense in basal cell nuclei **(Fig. 8, stars and insets)**.

359
360 **Presence of primary cilia components in the human epididymis**

361 In order to translate our observations made from a transgenic mouse model, we investigated
362 the expression of two primary cilia markers, Arl13b and IFT88, in human epididymal tissues **(Fig.**
363 **9, Supplementary file 5)**. We observed strong exogenous staining for Arl13b in the apical pole
364 of the epithelial cells from the proximal segment, corresponding to the *efferent ducts/caput*
365 **(Fig. 9, ED/caput inset)**. Whereas the signal was less intense in the *corpus* and *cauda*
366 epididymidis, it was mainly localized in peritubular myoid cells as well as in basal cells **(Fig. 9,**
367 **arrows in insets)**. An identical detection profile was observed for IFT88 **(Supplementary file 5)**.

368

369 Discussion

370 Primary cilia are solitary antennae found at the cell surface and are fundamental to organ
371 development and homeostasis [20]. Accordingly, impairment of primary cilia formation in
372 humans is responsible for a broad range of clinical syndromes—including male infertility—and
373 diseases referred to as ciliopathies [28-35]. While these organelles have been broadly studied in
374 most biological systems, investigations performed on primary cilia in the male reproductive
375 system remain scarce [18, 52]. Acknowledging the potential of primary cilia in the diagnosis of
376 unexplained male infertility, we portrayed for the first time the cell lineage specificity of primary
377 cilia in the epididymis, the organ of the male reproductive system in charge of post-testicular
378 sperm maturation (*i.e.* acquisition of motility and abilities to recognize and fertilize an egg) and
379 sustaining male fertility.

380 Almost every vertebrate cell has a primary cilium, which is a dynamic cell surface projection
381 playing the role of a sensory and signaling organelle. Although primary cilia were first described
382 by Ecker in 1844, knowledge of the full scope of their functions is continuously expanding with
383 the development of transgenic mouse models and the increasing number of human diseases
384 related to primary cilia dysfunctions [53]. With the re-appreciation of this biological antenna
385 over the past 10 years, it has become clear that the role of primary cilia in sensing the
386 extracellular environment potentially takes place in almost every cell responsive to intercellular
387 cross-talks and bodily fluid changes. The epididymis is a singular tubule that comprises distinct
388 segments, each controlling the composition of a dynamic epididymal fluid for proper sperm
389 maturation. Several mechanisms of intercellular communication between epididymal somatic
390 cells and between somatic and spermatogenic cells have been shown to be of major importance for
391 the control of sperm fertilizing abilities and reproductive outcomes [45, 50, 54-56]. We unveiled
392 here, for the first time, the existence of primary cilia displaying a cell lineage specificity and key
393 features of signaling antenna in the developing epididymis. In light of the spatio-temporal
394 changes of primary cilia observed during PND, and the functional components associated with
395 these antenna (*i.e.* PC1/PC2 and Gli3), we propose a novel mechanism of intercellular
396 communication involving primary cilia organelles in the control of epididymis development and
397 homeostasis (**Fig. 10**).

398 By using a transgenic mouse model developed to detect endogenous fluorescence in both ciliary
399 extension and centrioles, we determined that primary cilia were exclusively associated with
400 basal cells in the epididymal epithelium of adult mice. This is consistent with the serendipitous
401 observation made in 2013 by Arrighi, who documented the presence of primary cilia in the
402 epididymis of equine species [18]. In this unique article on epididymis primary cilia, typical 9+0
403 microtubular patterns and ciliary extensions were observed by transmission electron
404 microscopy associated with basal cells, according to their characteristic morphological features.
405 Our findings not only confirmed the cell specificity of primary cilia though co-localization of
406 primary cilia with keratin-5 positive basal cells, but also underscored a change in ciliary features
407 (length, orientation and signaling components) throughout the different segments of the
408 epididymis. Epididymal basal cells present with dynamic axiopodia extensions that cross the
409 blood-epididymis barrier to sense the lumen [49, 50]. According to our observations, the fact
410 that primary cilia never cross the apical tight junctions in adult epididymis— even when basal
411 cells present with elongated axiopodia—suggests that primary cilia might sense intra-epithelial
412 extracellular fluid rather than the intraluminal fluid in adult mice.

413 Basal cells from several other stratified and pseudo-stratified epithelia expose primary cilia with
414 distinct signaling functions. For instance, basal cells from the olfactory epithelium have primary
415 cilia that control basal cell activation, proliferation and differentiation, and as such are
416 necessary for regeneration of the epithelium following injury [57]. In addition, primary cilia
417 associated with basal cells from the mammary gland are involved in the acquisition of their stem
418 cell properties via Hh signaling, thereby controlling mammary tissue outgrowth and basal cell
419 tumor development [58]. While limited information is available with regard to basal cell
420 functions in the epididymis, their association with primary cilia could underlie a new functional
421 hypothesis related to epididymis development and homeostasis. According to gene expression
422 profiling, basal cells share common properties with adult stem cells and were recently proposed
423 to differentiate into columnar cells as a mechanism of epididymal epithelium regeneration [59].
424 Although basal cells from the epididymis do not seem to be progenitors of the other cell
425 populations during early development [14, 60], they may participate in epithelium regeneration
426 via primary cilia signaling, in a similar manner to other epithelia. In addition, primary cilia-

427 dependent control of tumorigenesis via Hh signaling appears to be common in cases of basal
428 cell carcinoma [61]. It is striking that the epididymis rarely develops tumors [62, 63]. Among the
429 few cases that have been described in the literature, two thirds of epididymal epithelial tumours
430 (papillary cystadenoma) are associated with Von Hippel-Lindau (VHL) syndrome, an atypical
431 ciliopathy[64]. Thus, it is possible that primary cilia monitor the epithelium stability of the
432 epididymis and prevent oncogenic events through Hh or Wnt signaling pathways, whose
433 downstream effectors are enriched in basal cells ([59] and our data).

434 Depending on the physiological context, primary cilia could exert dual sensory functions, either
435 as mechanosensors and/or chemosensors (For reviews, [19, 20, 65]). With regard to
436 chemosensing, the existence of transition fibers located at the base of the cilium physically
437 confines specialized molecules into the cilium, which potentiates signaling responses to
438 extracellular cues. Among these signals, primary cilia coordinate Hh, Wnt and PDGFR and signal-
439 transduction machineries. Interestingly, the components of these pathways—either agonists or
440 downstream effectors—are all found enriched in basal cells of the epididymis [59] and are
441 particularly relevant to the control of epididymis homeostasis and post-testicular maturation
442 events occurring in this organ [62, 66-71]. For instance, blockage of the Hh signaling pathway
443 following cyclopamine administration triggers a significant decrease in Gli1 and Gli3
444 transcriptional factor expression as well as a significant decrease in epididymal sperm motility
445 [69]. Whether or not this phenotype relies on primary cilia-dependent Hh signaling remains to
446 be established. Complementary *in vivo* studies on basal cell primary cilia will further define the
447 contribution of this organelle to epididymis physiology, and ultimately to sperm maturation and
448 male fertility.

449 Finally, the fact that primary cilia are observed at the apical pole of the epithelium from early
450 stages of PND to puberty and colocalize with polycystins (PC1 and PC2), suggests that these
451 organelles might play the role of mechanosensors before puberty. This type of primary cilia-
452 dependent mechanosignaling is broadly documented in the kidney, which shares the same
453 embryonic origin as the epididymis and presents numerous functional similarities with it [24,
454 26]. In epithelial cells from the distal convoluted and connecting tubules of the kidney, the flow
455 shear stress exerted at the surface of the cells is sensed by primary cilia exposed at the cell

456 surface. The subsequent physical bending of primary cilia triggers PC1 dependent-transepithelial
457 transport of calcium and controls tissue morphogenesis [26]. Approximately 40 years ago, Sun
458 and Flickinger proposed that the flow of testicular-derived fluid entering the epididymis before
459 sperm production may stimulate epithelial cell proliferation and differentiation in the
460 epididymis [1]. Building on our new findings, it is now conceivable that primary cilia are
461 strategically positioned in direct contact with the lumen of the epididymis to initiate shear-flow
462 dependent epithelium maturation and sense the first wave of spermatozoa at puberty to
463 sustain maturation.

464 In conclusion, our study reveals for the first time the cell lineage specificity of primary cilia along
465 the epididymis at different stages of PND. Acknowledging the important role played by these
466 sensory organelles in most biological systems, our work opens new avenues of research
467 concerning the cellular control of epididymal development and homeostasis. Importantly, since
468 primary cilia components are conserved in the human epididymis, current drugs controlling
469 ciliary functions might constitute new targets for the development of non-hormonal male
470 contraceptives or treatments for cases of unexplained male infertility.

471

472 **Acknowledgements**

473 We thank Pr Sylvie Breton, Ph.D., for providing aquaporin 9 antibody used in this project, as well
474 as Pr Marie-Claire Orgebin-Crist, Ph.D., for providing epididymal DC2 cell line. We would like to
475 acknowledge the contribution of Sabine Elowe, Ph.D., for confocal imaging support, Robert
476 Sullivan, Ph.D., for giving us access to the biobank of human tissues, and Christine Légaré, M.Sc.,
477 for her technical support. The contributions of Johanne Ouellet in histology services, France
478 Couture in illustration and Julie-Christine Lévesque, M.Sc., from the bio-imagery core facility are
479 also acknowledged. Enthusiastic informal discussions with Rex Ress, Ph.D. were highly
480 appreciated throughout this project.

481

482 **Competing interests**

483 The authors declare no competing or financial interests.

484

485 **Author contributions**

486 Experiments were conceived and designed by ABa, ABe, CB, CRoy, and DS. Contributed to
487 critical reagent, resources and expertise; CB, CRo, DS, JB, MET. Experiments were performed by
488 ABa, ABe, CB, CL, CRoy, DS, OJ, MBR. Data were processed and analyzed by ABa, ABe, CB, CRoy,
489 DS, MBR, and supervised by CB, CRo, DS, JB, and MET. The manuscript was written by ABe, CRoy
490 and CB, and critically reviewed by all authors.

491

492 **Funding support**

493 This work was supported by a NSERC operating grant (RGPIN-2015-109194) and a FRQS-Junior 1
494 salary award to CB, NSERC grant to MET (RGPIN-2014-05308), NSERC grant to CRo (RGPIN-2017-
495 04775), and a FRQS-Junior 2 career award and CFI equipment to DS. ABe is recipient of a CRDSI
496 fellowship. MBR is recipient of a FAPESP fellowship. CL is recipient of a FRQS master award
497 scholarship. MET is a Canada Research Chair (Tier 2) in *Neuroimmune Plasticity in Health and*
498 *Therapy*.

499 **Figure legends**

500

501 **Fig. 1. Detection of primary cilia in Arl13b-Cetn2 tg mice.** Epididymal sections from Arl13b-
502 Cetn2 tg mice **(A)** were stained for the primary cilia marker acetylated tubulin (Ac-Tub) **(B)**.
503 Arl13b-positive cilia extensions colocalize with Ac-Tub **(Arrows, A, B and C)**, which validates this
504 mouse model for the study of primary cilia in the epididymis. Ep.: epithelium; Lu.: lumen; Mc.:
505 myoid cells. Scale bar: 10 μ m.

506

507 **Fig. 2. Primary cilia extend from basal and peritubular myoid cells in the epididymis of adult**
508 **mice.** Immunofluorescent staining for alpha-actin myoid cell marker **(A and inset)**, aquaporin 9
509 (Aqp9) principal cell marker **(C)**, keratin-5 (Krt5) basal cell marker **(D and inset)** was performed
510 on epididymal sections from Arl13b-Cetn2 dTg mice. Primary cilia structural components were
511 detected by transmission electron microscopy in epididymal peritubular myoid cells from
512 C57BL/6 mice **(B)**. Ax.: axoneme; Bb.: basal body; Ct.: connective tissue; Lu.: lumen; Mc.: myoid
513 cells.

514

515 **Fig. 3. Primary cilia extend from basal cells' main body.** Confocal acquisition of the initial
516 segment from the epididymis of Arl13b-Cetn2 dTg mice showing a ciliated basal cell. Arl13b-
517 positive primary cilia extend from centrin2-positive centrioles located at the base of the
518 axiopodia (Axp.).

519

520 **Fig. 4. Primary cilia are observed in the efferent ducts (ED), the vas deferens (VD), and the**
521 **different segments of the mouse epididymis.** Primary cilia were observed associated with basal
522 cells (stars) and peritubular myoid cells in all segments of the epididymis **(A)**. The angle of basal
523 cell primary cilia relative to the closest tubule edge was determined by image processing in each
524 epididymal region, *i.e.* IS/Caput (n=899 cells), corpus (n=371 cells) and cauda (n=1065 cells) from
525 3 mice. Proportions of primary cilia with distinct angles were distributed between -90° for cilia
526 directed towards the base of the epithelium to 90° for cilia directed towards the lumen **(B)**. Ep.:
527 epithelium. Lu.: Lumen. Mc.: myoid cell. IS: initial segment. Scale bars: 10 μ m.

528

529 **Fig. 5. Primary cilia are observed at different stages of epididymis post-natal development.**

530 Hematoxylin and eosin staining (H & E) and confocal imaging were performed on epididymis
531 sections from Arl13b-Cetn2 dTg mice at different stages of post-natal development, *i.e.* at 5, 30,
532 42 and 268 dpn. Schematic representation of primary cilia location is shown throughout post-
533 natal development with centrioles displayed in green and primary cilia in red. NDC: non-
534 differentiated cells; DC: differentiated cells; MC: myoid cells; Lu.: lumen.

535

536 **Fig. 6. Primary cilia are in contact with the intraluminal compartment of the epididymis at an
537 early stage of post-natal development.** Immunofluorescent staining for the tight junction

538 protein-1 (ZO1) on the cauda epididymidis of Arl13b-Cetn2 dTg mice at 5 dpn. Lu.:lumen;
539 Ep.:epithelium.

540

541 **Fig. 7. Expression of Polycystin1 (PC1) and Polycystin 2 (PC2) in epididymal cells and in the
542 mouse epididymis. (A)** Immunohistochemical staining for PC1 on the epididymis of Arl13b-
543 Cetn2 dTg mice at 7 and 40 dpn. Cap.: caput; Cor.:corpus; Cau.:cauda; VD: *Vas deferens*. Scale
544 bar: 50 μ m. **(B)** Immunofluorescent staining for PC2 and the primary cilia marker acetylated
545 tubulin (Ac-Tub) in DC2 cells.

546

547 **Fig. 8. Expression of Gli3 in the mouse epididymis.** Immunohistochemical staining for Gli3 on
548 the epididymis of Arl13b-Cetn2 dTg mice at 40 dpn. P-Cap: proximal caput; D-Cap: distal caput;
549 Cor.:corpus; Cau.:cauda. Inset scale bar: 10 μ m

550

551 **Fig. 9. Expression of Arl13b in the human epididymis.** Immunohistochemical staining for Arl13b
552 was performed on the different segments of a human epididymis (donor age = 50).

553

554 **Fig. 10. Cell lineage specificity and potential roles of primary cilia in the epididymis during
555 postnatal development.** Potential mechano/chemo-sensory functions associated with epithelial
556 cells primary cilia are presented.

557 **Supplementary files.**

558 **Supplementary file 1.** 3D reconstruction of the epididymal epithelium after ZO-1 staining in
559 adult Arl13b-Cetn2 tg mice

560 **Supplementary file 2.** Proportion of primary cilia found in basal and myoid cells from different
561 epididymal segments.

562 **Supplementary file 3.** 3D reconstruction of the epididymal epithelium in Arl13b-Cetn2 tg mice
563 at early stage of PND (at 5 dpn).

564 **Supplementary file 4.** 3D reconstruction of the epididymal epithelium in Arl13b-Cetn2 tg mice
565 after puberty (at 40 dpn).

566 **Supplementary file 5.** Immunohistochemistry staining for IFT88 in human epididymis.

567

568

569 **Table 1. List of antibodies used in our study.**

Type	Name	Host species	Dilution	Antigen retrieval	IHC	Company	Catalog number
polyclonal	Cytokeratin5	rabbit	1-250	no		Abcam	ab53121
polyclonal	AQP9	rabbit	1-500	no		N/A	N/A
monoclonal	ZO-1	mouse	1-100	no		ThermoFisher	ZO1-1A12
polyclonal	α -actin	rabbit	1-100	no		Abcam	ab5694
polyclonal	Arl13b	rabbit	1-50	no		Proteintech	17711-1-AP
monoclonal	Acetylated tubulin	mouse	1-250	no		Sigma	T7451
polyclonal	IFT88	rabbit	1-200	no		Proteintech	13967-1-AP
polyclonal	PC1	rabbit	1-100	no		Bioss	2157R
polyclonal	PC2	rabbit	1-400	no		Bioss	2158R
monoclonal	Shh	rabbit	1-500		citrate buffer	Abcam	ab53281
monoclonal	Ihh	rabbit	1-100	no		Abcam	ab52919

570

571

572

573

574

575

576

577

578

579

580

581

582

583

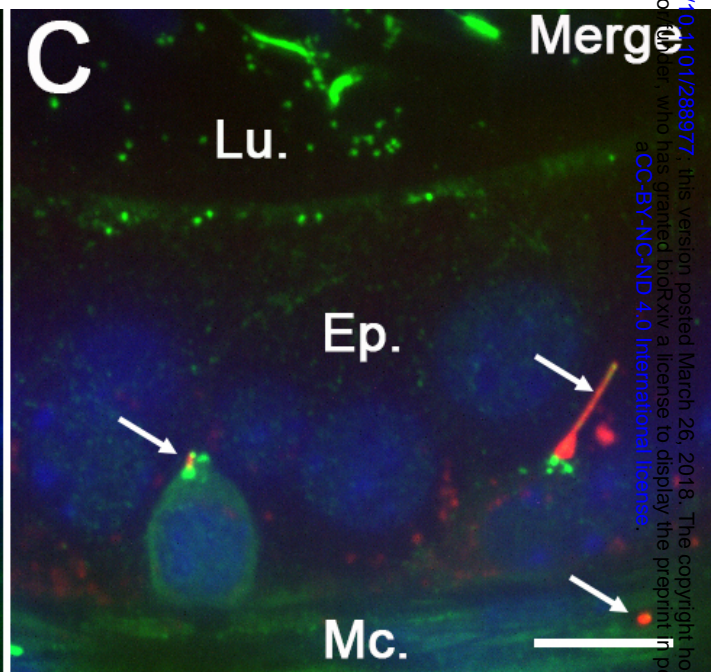
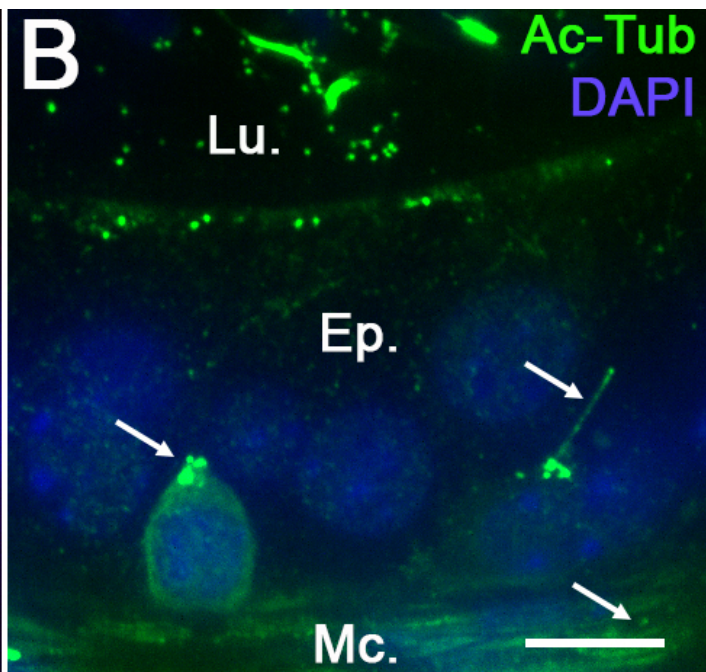
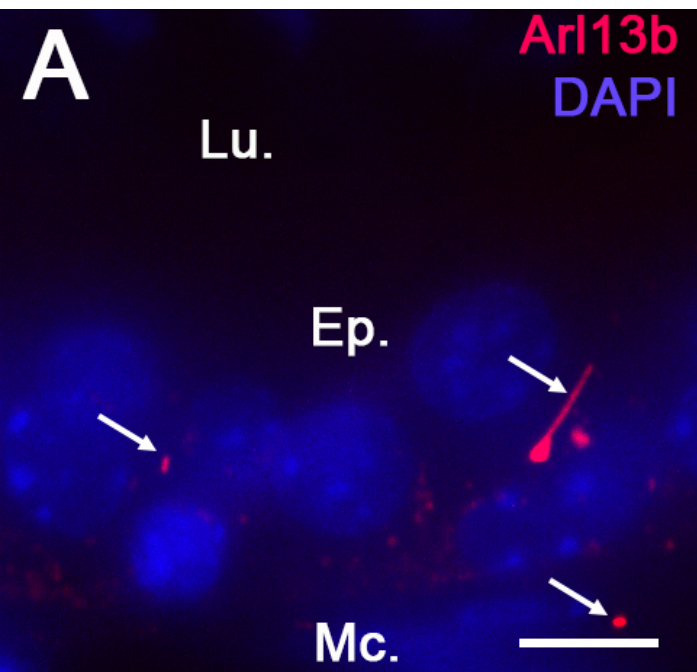
584 **References.**

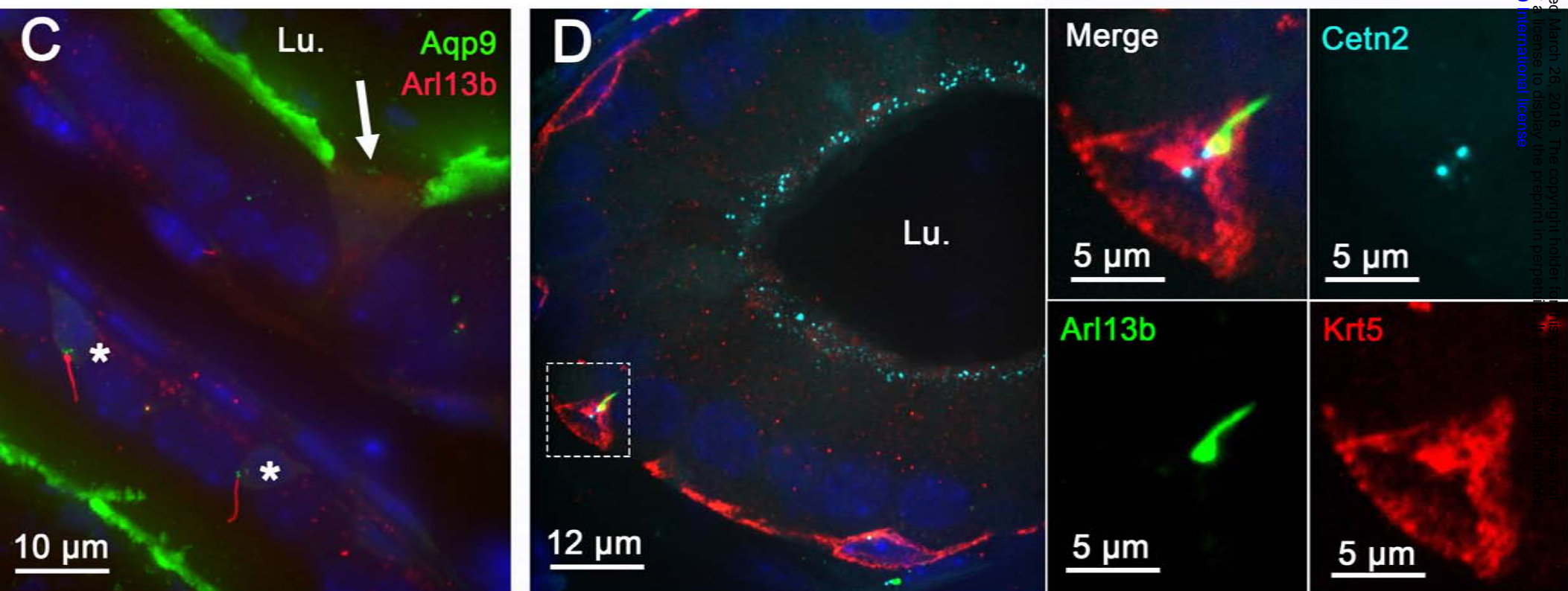
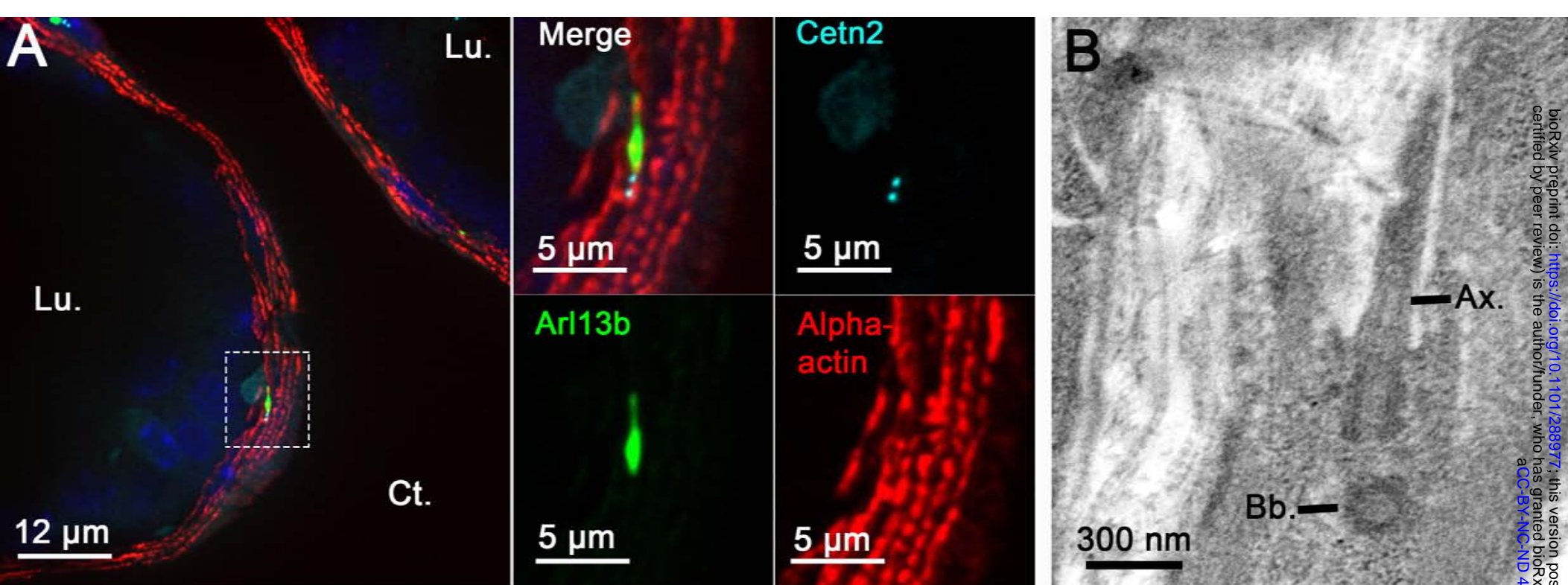
- 585 1. Sun, E.L., et al., *Development of cell types and of regional differences in the postnatal*
586 *rat epididymis*. Am J Anat, 1979. **154**(1): p. 27-55.
- 587 2. Rodriguez, C.M., et al., *The development of the epididymis*, in *The epididymis: from*
588 *molecules to clinical practices*, R.a. Hinton, Editor. 2002, Kluwer Academic/Plenum
589 Publishers. p. 251-267.
- 590 3. Belleannée, C., et al., *Region-specific gene expression in the epididymis*. Cell Tissue Res,
591 2012.
- 592 4. Suzuki, F., et al., *Regional differentiation of cell junctions in the excurrent duct*
593 *epithelium of the rat testis as revealed by freeze-fracture*. Anat Rec, 1978. **191**(4): p.
594 503-19.
- 595 5. Suzuki, F., et al., *Development of tight junctions in the caput epididymal epithelium of*
596 *the mouse*. Dev Biol, 1978. **63**(2): p. 321-34.
- 597 6. Takano, H., *[Qualitative and quantitative histology and histogenesis of the mouse*
598 *epididymis, with special emphasis on the regional difference (author's transl)]*.
599 Kaibogaku Zasshi, 1980. **55**(6): p. 573-87.
- 600 7. Abe, K., et al., *Interruption of the luminal flow in the epididymal duct of the corpus*
601 *epididymidis in the mouse, with special reference to differentiation of the epididymal*
602 *epithelium*. Arch Histol Jpn, 1984. **47**(2): p. 137-47.
- 603 8. Abe, K., et al., *Ultrastructure of the mouse epididymal duct with special reference to the*
604 *regional differences of the principal cells*. Arch Histol Jpn, 1983. **46**(1): p. 51-68.
- 605 9. Abe, K., et al., *Response of the epididymal duct in the corpus epididymidis to efferent or*
606 *epididymal duct ligation in the mouse*. J Reprod Fertil, 1982. **64**(1): p. 69-72.
- 607 10. Zondek, L.H., et al., *Normal and abnormal development of the epididymis of the fetus*
608 *and infant*. Eur J Pediatr, 1980. **134**(1): p. 39-44.
- 609 11. Francavilla, S., et al., *Postnatal development of epididymis and ductus deferens in the*
610 *rat. A correlation between the ultrastructure of the epithelium and tubule wall, and the*
611 *fluorescence-microscopic distribution of actin, myosin, fibronectin, and basement*
612 *membrane*. Cell Tissue Res, 1987. **249**(2): p. 257-65.
- 613 12. Tajiri, S., et al., *Changes in lectin-binding sites on epididymal cells during postnatal*
614 *development of the mouse*. Okajimas Folia Anat Jpn, 2012. **88**(4): p. 153-7.
- 615 13. Hermo, L., et al., *Epithelial cells of the epididymis show regional variations with respect*
616 *to the secretion of endocytosis of immobilin as revealed by light and electron*
617 *microscope immunocytochemistry*. Anat Rec, 1992. **232**(2): p. 202-20.
- 618 14. Shum, W.W., et al., *Plasticity of basal cells during postnatal development in the rat*
619 *epididymis*. Reproduction, 2013. **146**(5): p. 455-69.
- 620 15. Alexander, N.J., *Prenatal development of the ductus epididymidis in the rhesus monkey.*
621 *The effects of fetal castration*. Am J Anat, 1972. **135**(1): p. 119-34.
- 622 16. Orgebin-Crist, M.C., et al., *The effects of estradiol, tamoxifen, and testosterone on the*
623 *weights and histology of the epididymis and accessory sex organs of sexually immature*
624 *rabbits*. Endocrinology, 1983. **113**(5): p. 1703-15.
- 625 17. Robaire B, H.L., *Efferent ducts, epididymis, and vas deferens: structure, functions and*
626 *their regulation.*, in *The physiology of reproduction*, O.N.J. Knobil E, Editor. 1988,
627 Raven press: New York. p. 999-1080.
- 628 18. Arrighi, S., *Primary cilia in the basal cells of equine epididymis: a serendipitous finding.*
629 *Tissue Cell*, 2013. **45**(2): p. 140-4.

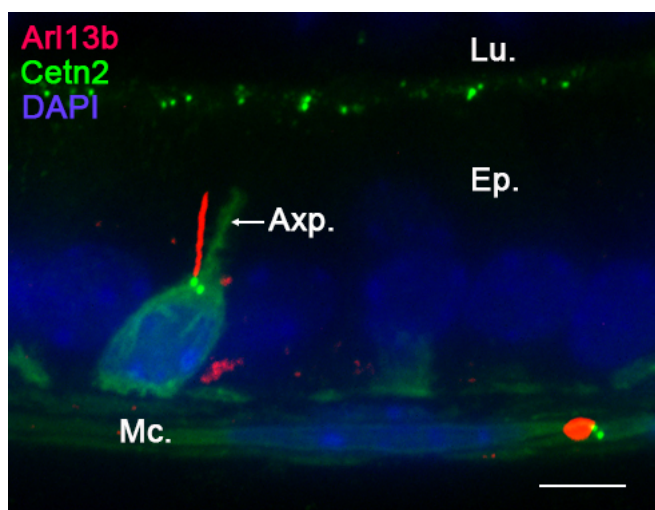
- 630 19. Satir, P., et al., *The primary cilium at a glance*. J Cell Sci, 2010. **123**(Pt 4): p. 499-503.
- 631 20. Singla, V., et al., *The primary cilium as the cell's antenna: signaling at a sensory*
- 632 *organelle*. Science, 2006. **313**(5787): p. 629-33.
- 633 21. Bangs, F., et al., *Primary Cilia and Mammalian Hedgehog Signaling*. Cold Spring Harb
- 634 *Perspect Biol*, 2017. **9**(5).
- 635 22. Grisanti, L., et al., *Primary cilia maintain corneal epithelial homeostasis by regulation*
- 636 *of the Notch signaling pathway*. Development, 2016. **143**(12): p. 2160-71.
- 637 23. Clement, D.L., et al., *PDGFRalpha signaling in the primary cilium regulates NHE1-*
- 638 *dependent fibroblast migration via coordinated differential activity of MEK1/2-*
- 639 *ERK1/2-p90RSK and AKT signaling pathways*. J Cell Sci, 2013. **126**(Pt 4): p. 953-65.
- 640 24. Mohammed, S.G., et al., *Fluid shear stress increases transepithelial transport of Ca²⁺ in*
- 641 *ciliated distal convoluted and connecting tubule cells*. FASEB J, 2017. **31**(5): p. 1796-
- 642 1806.
- 643 25. Praetorius, H.A., *The primary cilium as sensor of fluid flow: new building blocks to the*
- 644 *model. A review in the theme: cell signaling: proteins, pathways and mechanisms*. Am J
- 645 *Physiol Cell Physiol*, 2015. **308**(3): p. C198-208.
- 646 26. Nauli, S.M., et al., *Polycystins 1 and 2 mediate mechanosensation in the primary cilium*
- 647 *of kidney cells*. Nat Genet, 2003. **33**(2): p. 129-37.
- 648 27. Bangs, F.K., et al., *Lineage specificity of primary cilia in the mouse embryo*. Nat Cell
- 649 *Biol*, 2015. **17**(2): p. 113-22.
- 650 28. Hildebrandt, F., et al., *Ciliopathies*. N Engl J Med, 2011. **364**(16): p. 1533-43.
- 651 29. Belet, U., et al., *Prevalence of epididymal, seminal vesicle, prostate, and testicular cysts*
- 652 *in autosomal dominant polycystic kidney disease*. Urology, 2002. **60**(1): p. 138-41.
- 653 30. Kanagarajah, P., et al., *Male infertility and adult polycystic kidney disease--revisited:*
- 654 *case report and current literature review*. Andrologia, 2012. **44 Suppl 1**: p. 838-41.
- 655 31. van der Linden, E.F., et al., *Polycystic kidney disease and infertility*. Fertil Steril, 1995.
- 656 **64**(1): p. 202-3.
- 657 32. Frantzen, C., et al., *Von Hippel-Lindau Syndrome*, in *GeneReviews((R))*, M.P. Adam, et
- 658 al., Editors. 1993: Seattle (WA).
- 659 33. Chou, A., et al., *von Hippel-Lindau syndrome*. Front Horm Res, 2013. **41**: p. 30-49.
- 660 34. Crespigio, J., et al., *Von Hippel-Lindau disease: a single gene, several hereditary tumors*.
- 661 *J Endocrinol Invest*, 2018. **41**(1): p. 21-31.
- 662 35. Glasker, S., et al., *Epididymal cystadenomas and epithelial tumourlets: effects of VHL*
- 663 *deficiency on the human epididymis*. J Pathol, 2006. **210**(1): p. 32-41.
- 664 36. Miyoshi, K., et al., *Lack of dopaminergic inputs elongates the primary cilia of striatal*
- 665 *neurons*. PLoS One, 2014. **9**(5): p. e97918.
- 666 37. Miyoshi, K., et al., *Factors that influence primary cilium length*. Acta Med Okayama,
- 667 **65**(5): p. 279-85.
- 668 38. Miyoshi, K., et al., *Lithium treatment elongates primary cilia in the mouse brain and in*
- 669 *cultured cells*. Biochem Biophys Res Commun, 2009. **388**(4): p. 757-62.
- 670 39. Miyoshi, K., et al., *Pericentrin, a centrosomal protein related to microcephalic*
- 671 *primordial dwarfism, is required for olfactory cilia assembly in mice*. FASEB J, 2009.
- 672 **23**(10): p. 3289-97.
- 673 40. Toriyama, M., et al., *Folate-dependent methylation of septins governs ciliogenesis*
- 674 *during neural tube closure*. FASEB J, 2017. **31**(8): p. 3622-3635.

- 675 41. Belleannee, C., et al.,*Role of microRNAs in controlling gene expression in different*
676 *segments of the human epididymis*. PLoS One, 2012. **7**(4): p. e34996.
- 677 42. Belleannée, C., et al.,*Segmental expression of the bradykinin type 2 receptor in rat*
678 *efferent ducts and epididymis and its role in the regulation of aquaporin 9*. Biol
679 *Reprod*, 2009. **80**(1): p. 134-43.
- 680 43. Bisht, K., et al.,*Dark microglia: A new phenotype predominantly associated with*
681 *pathological states*. *Glia*, 2016.
- 682 44. Araki, Y., et al.,*Immortalized epididymal cell lines from transgenic mice overexpressing*
683 *temperature-sensitive simian virus 40 large T-antigen gene*. *J Androl*, 2002. **23**(6): p.
684 854-69.
- 685 45. Belleannée, C., et al.,*Role of purinergic signaling pathways in V-ATPase recruitment to*
686 *apical membrane of acidifying epididymal clear cells*. *Am J Physiol Cell Physiol*, 2010.
687 **298**(4): p. C817-30.
- 688 46. Rueden, C.T., et al.,*ImageJ2: ImageJ for the next generation of scientific image data*.
689 *BMC Bioinformatics*, 2017. **18**(1): p. 529.
- 690 47. Chalfoun, J., et al.,*MIST: Accurate and Scalable Microscopy Image Stitching Tool with*
691 *Stage Modeling and Error Minimization*. *Sci Rep*, 2017. **7**(1): p. 4988.
- 692 48. Legare, C., et al.,*Expression and localization of c-ros oncogene along the human*
693 *excurrent duct*. *Mol Hum Reprod*, 2004. **10**(9): p. 697-703.
- 694 49. Roy, J., et al.,*Tyrosine kinase-mediated axial motility of basal cells revealed by*
695 *intravital imaging*. *Nat Commun*, 2016. **7**: p. 10666.
- 696 50. Shum, W.W., et al.,*Transepithelial projections from basal cells are luminal sensors in*
697 *pseudostratified epithelia*. *Cell*, 2008. **135**(6): p. 1108-17.
- 698 51. Domeniconi, R.F., et al.,*Is the Epididymis a Series of Organs Placed Side By Side?* *Biol*
699 *Reprod*, 2016. **95**(1): p. 10.
- 700 52. Does, C., et al.,*Primary cilia on porcine testicular somatic cells and their role in*
701 *hedgehog signaling and tubular morphogenesis in vitro*. *Cell Tissue Res*, 2017.
702 **368**(1): p. 215-223.
- 703 53. Tobin, J.L., et al.,*The nonmotile ciliopathies*. *Genet Med*, 2009. **11**(6): p. 386-402.
- 704 54. Jerczynski, O., et al.,*Role of Dicer1-Dependent Factors in the Paracrine Regulation of*
705 *Epididymal Gene Expression*. PLoS One, 2016. **11**(10): p. e0163876.
- 706 55. Belleannée, C., et al.,*Epididymosomes Convey Different Repertoires of MicroRNAs*
707 *Throughout the Bovine Epididymis*. *Biol Reprod*, 2013.
- 708 56. Sharma, U., et al.,*Biogenesis and function of tRNA fragments during sperm maturation*
709 *and fertilization in mammals*. *Science*, 2016. **351**(6271): p. 391-6.
- 710 57. Joiner, A.M., et al.,*Primary Cilia on Horizontal Basal Cells Regulate Regeneration of the*
711 *Olfactory Epithelium*. *J Neurosci*, 2015. **35**(40): p. 13761-72.
- 712 58. Guen, V.J., et al.,*EMT programs promote basal mammary stem cell and tumor-*
713 *initiating cell stemness by inducing primary ciliogenesis and Hedgehog signaling*. *Proc*
714 *Natl Acad Sci U S A*, 2017.
- 715 59. Mandon, M., et al.,*Isolated Rat Epididymal Basal Cells Share Common Properties with*
716 *Adult Stem Cells*. *Biol Reprod*, 2015. **93**(5): p. 115.
- 717 60. Murashima, A., et al.,*Essential roles of androgen signaling in Wolffian duct*
718 *stabilization and epididymal cell differentiation*. *Endocrinology*, 2011. **152**(4): p.
719 1640-51.

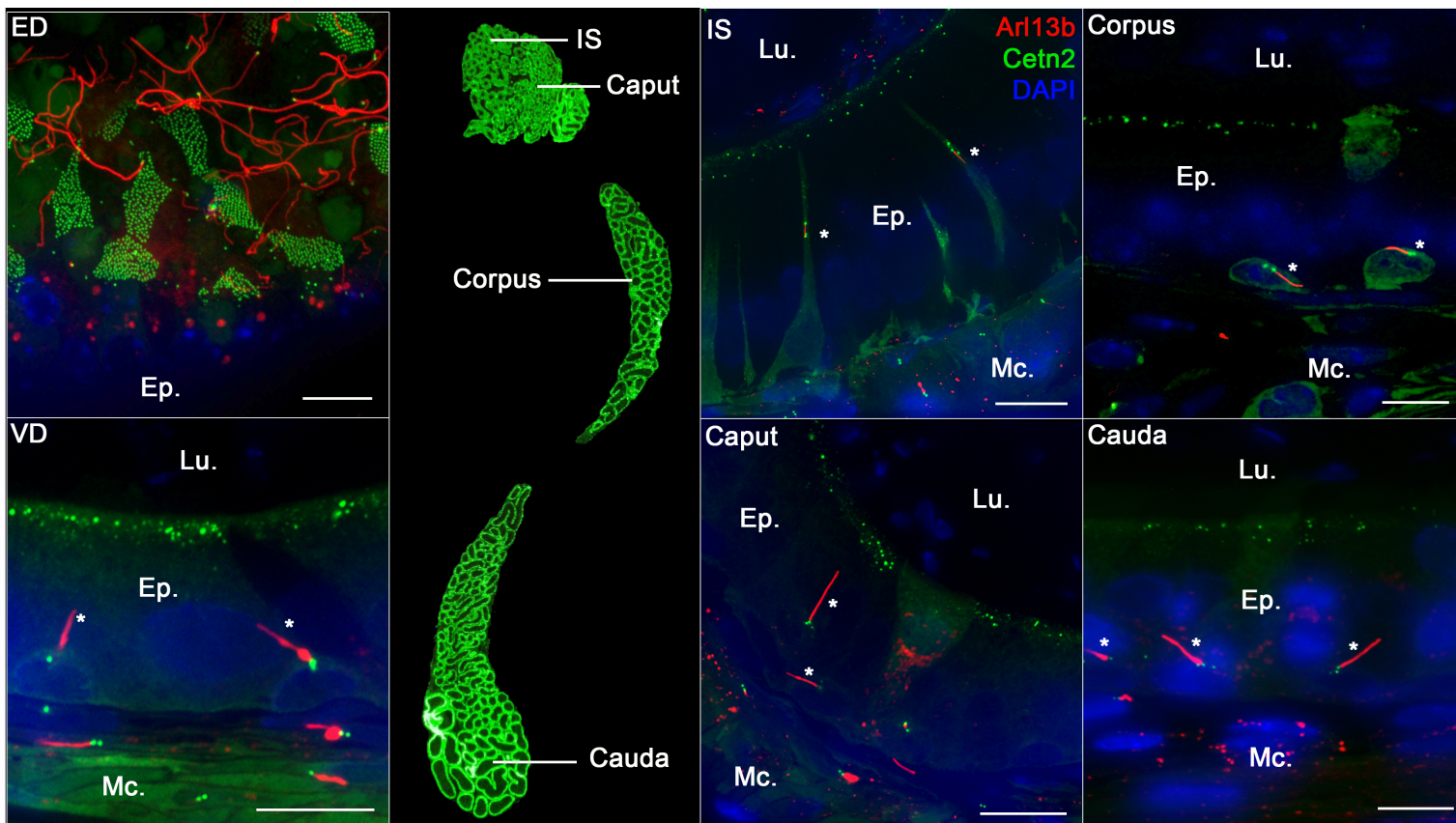
- 720 61. Wong, S.Y., et al., *Primary cilia can both mediate and suppress Hedgehog pathway-*
721 *dependent tumorigenesis.* Nat Med, 2009. **15**(9): p. 1055-61.
- 722 62. Wang, K., et al., *Oncogenic Wnt/beta-catenin signalling pathways in the cancer-*
723 *resistant epididymis have implications for cancer research.* Mol Hum Reprod, 2013.
724 **19**(2): p. 57-71.
- 725 63. Yeung, C.H., et al., *Why are epididymal tumours so rare?* Asian J Androl, 2012. **14**(3): p.
726 465-75.
- 727 64. Price, E.B., Jr., *Papillary cystadenoma of the epididymis. A clinicopathologic analysis of*
728 *20 cases.* Arch Pathol, 1971. **91**(5): p. 456-70.
- 729 65. Satir, P., *CILIA: before and after.* Cilia, 2017. **6**: p. 1.
- 730 66. Kumar, M., et al., *Epithelial Wnt/betacatenin signalling is essential for epididymal*
731 *coiling.* Dev Biol, 2016. **412**(2): p. 234-49.
- 732 67. Wang, K., et al., *Comparison of gene expression of the oncogenic Wnt/beta-catenin*
733 *signaling pathway components in the mouse and human epididymis.* Asian J Androl,
734 2015. **17**(6): p. 1006-11.
- 735 68. Koch, S., et al., *Post-transcriptional Wnt Signaling Governs Epididymal Sperm*
736 *Maturation.* Cell, 2015. **163**(5): p. 1225-36.
- 737 69. Turner, T.T., et al., *Sonic hedgehog pathway inhibition alters epididymal function as*
738 *assessed by the development of sperm motility.* J Androl, 2006. **27**(2): p. 225-32.
- 739 70. Turner, T.T., et al., *Sonic hedgehog pathway genes are expressed and transcribed in the*
740 *adult mouse epididymis.* J Androl, 2004. **25**(4): p. 514-22.
- 741 71. Basciani, S., et al., *Expression of platelet-derived growth factor (PDGF) in the*
742 *epididymis and analysis of the epididymal development in PDGF-A, PDGF-B, and PDGF*
743 *receptor beta deficient mice.* Biol Reprod, 2004. **70**(1): p. 168-77.
- 744



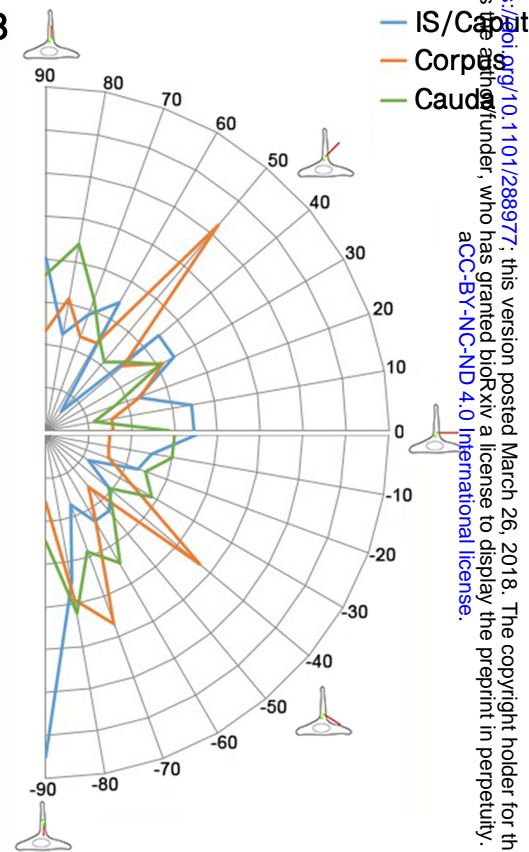




A

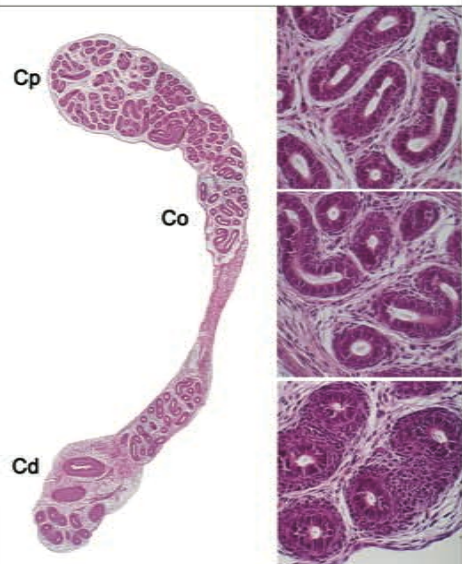


B

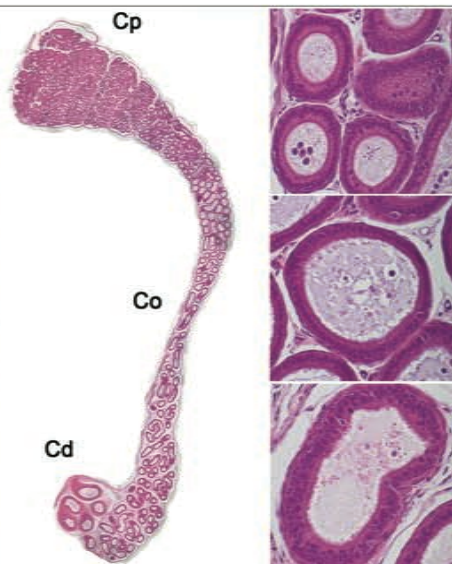


H & E staining

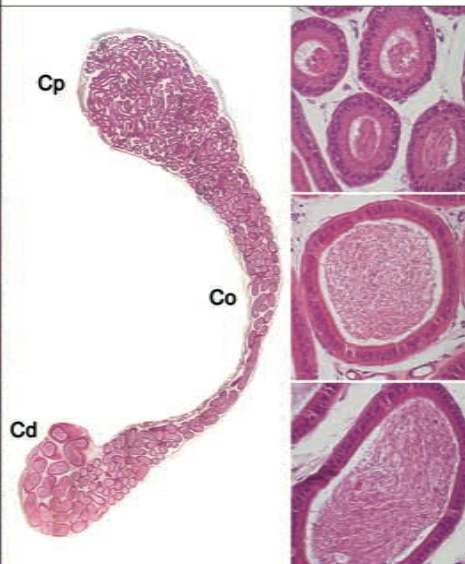
PND5



PND30



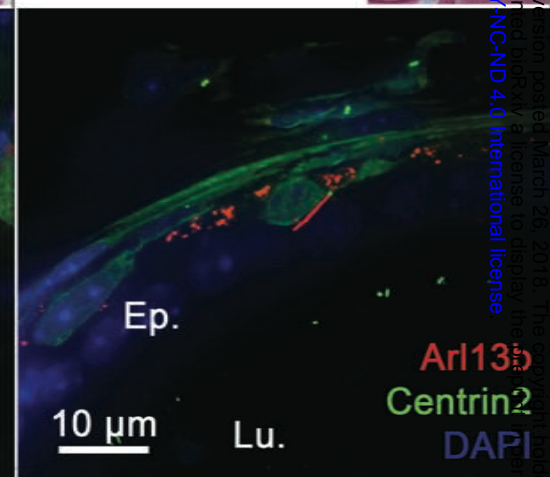
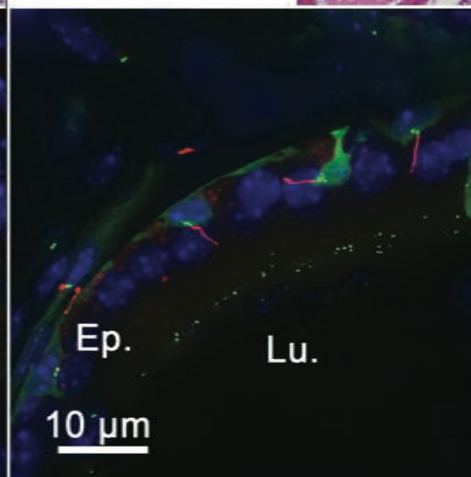
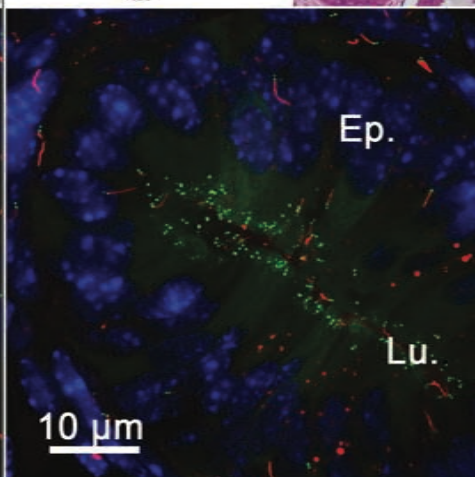
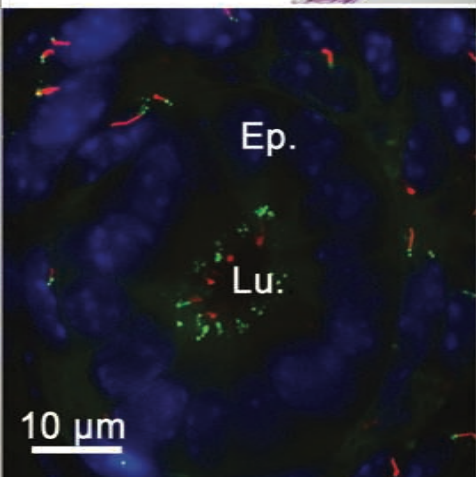
PND42



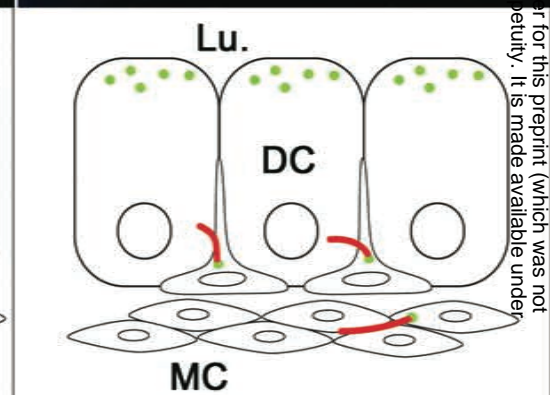
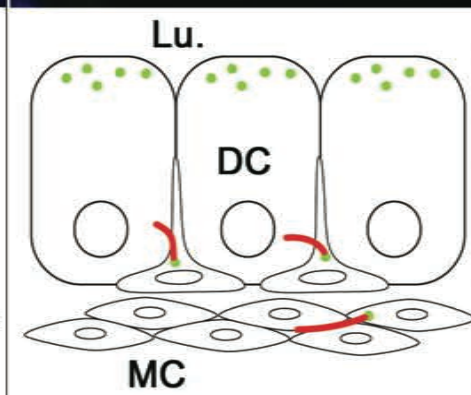
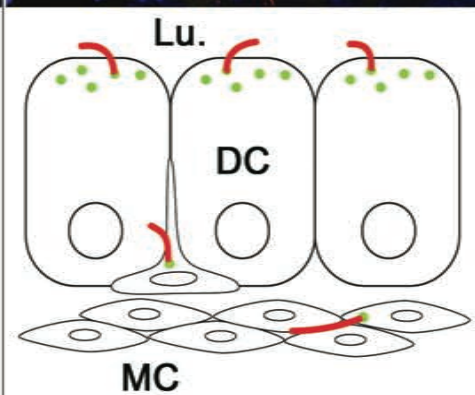
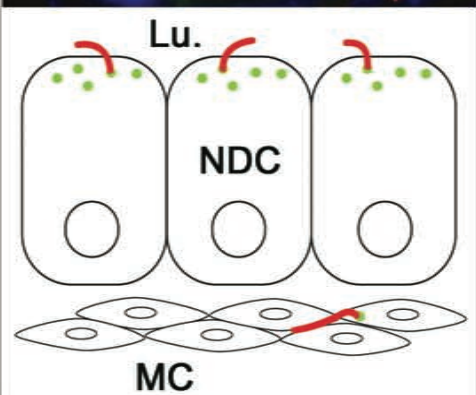
PND268



Confocal imaging



Schematic view

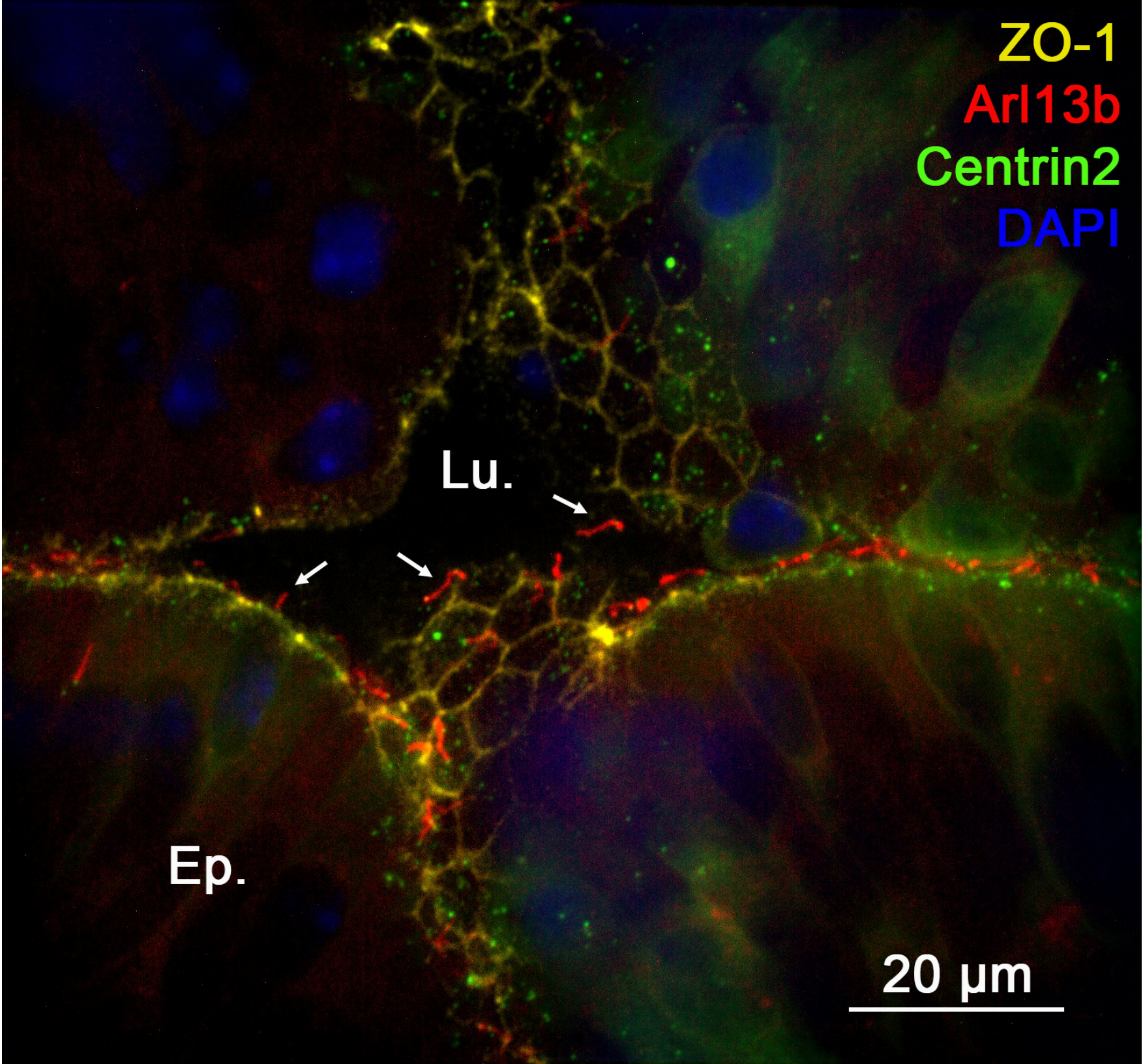


ZO-1

Arl13b

Centrin2

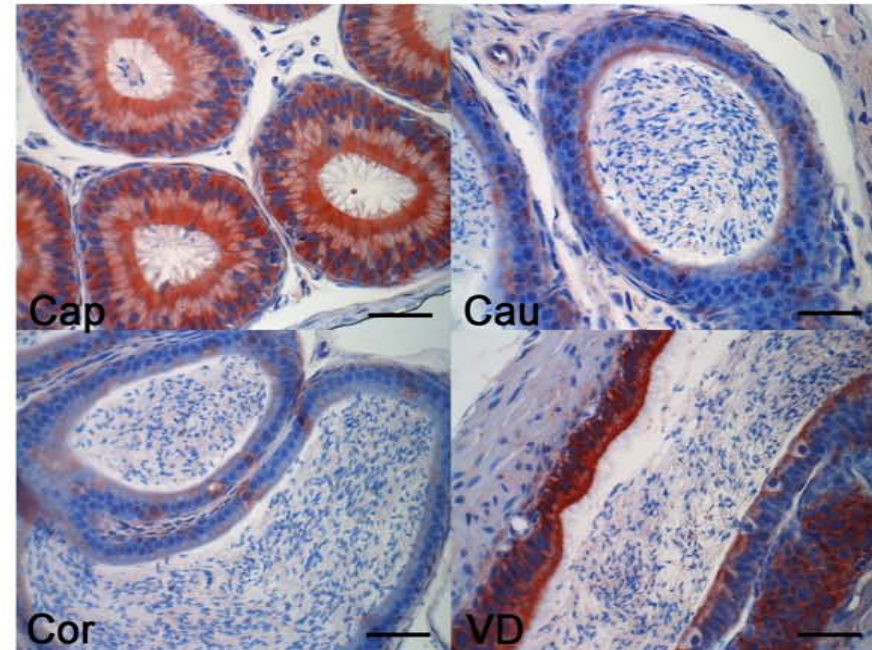
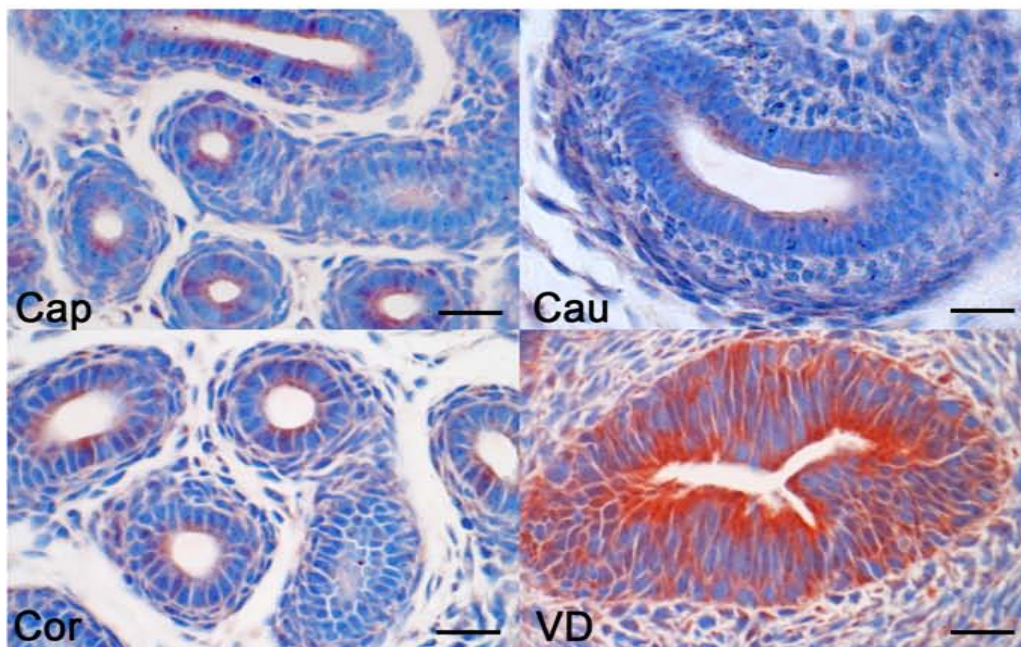
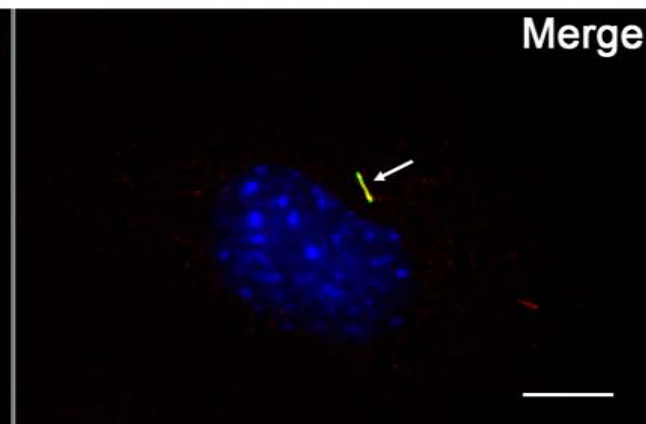
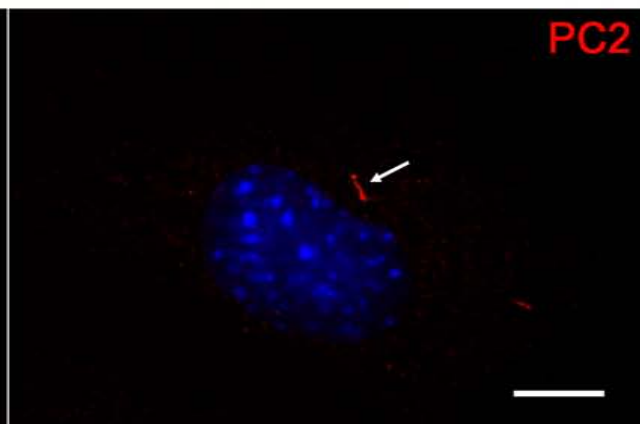
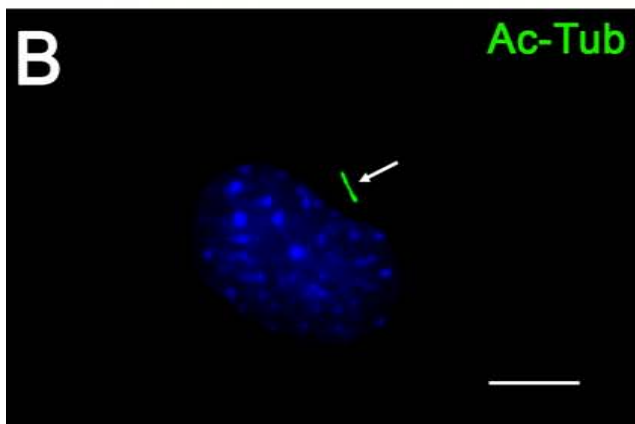
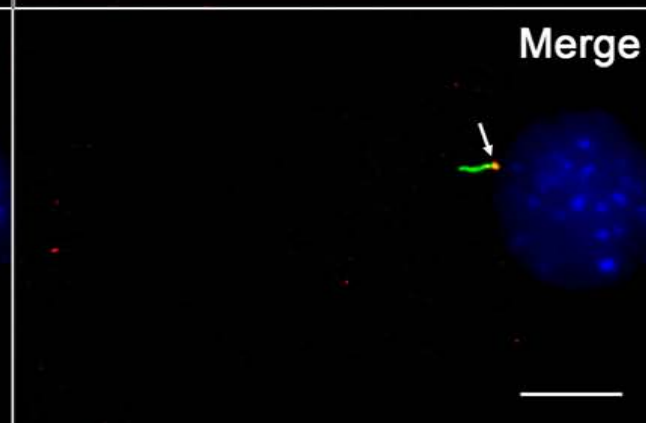
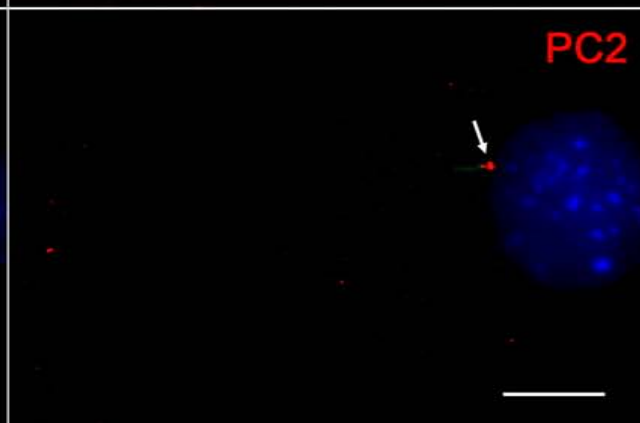
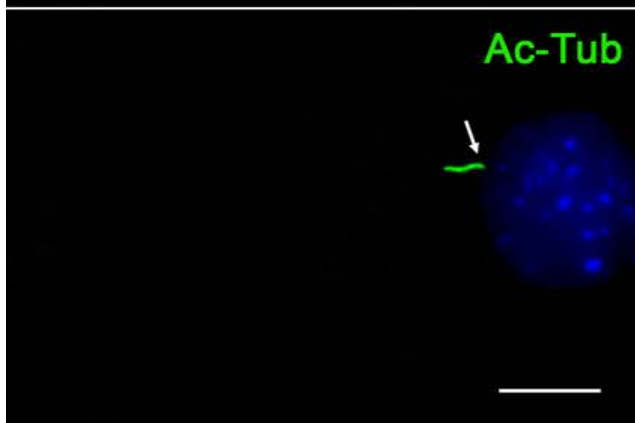
DAPI

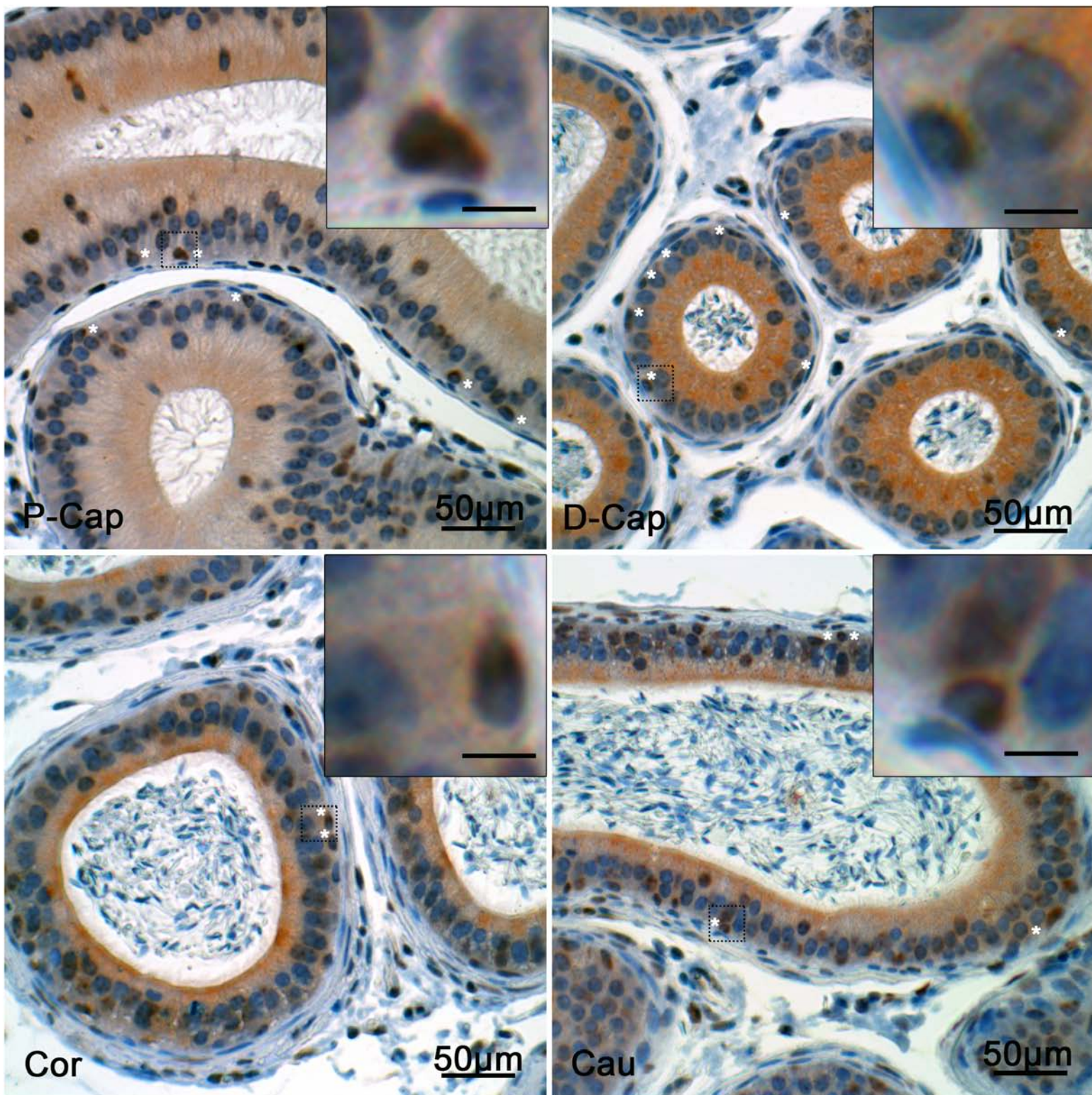


Lu.

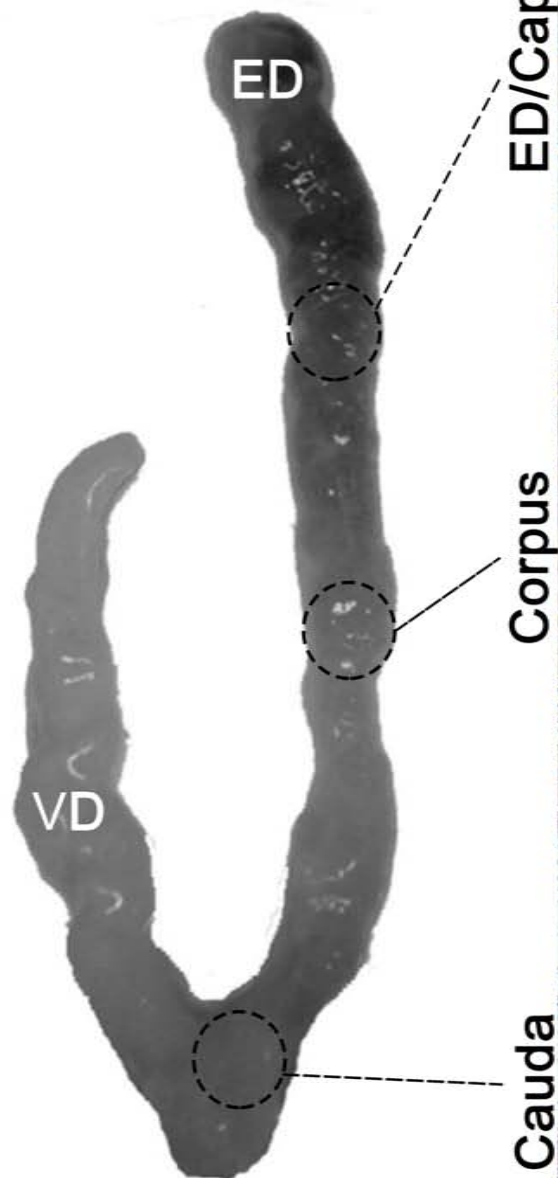
Ep.

20 μm

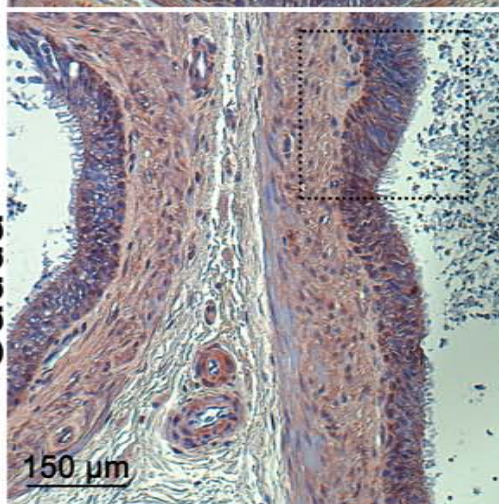
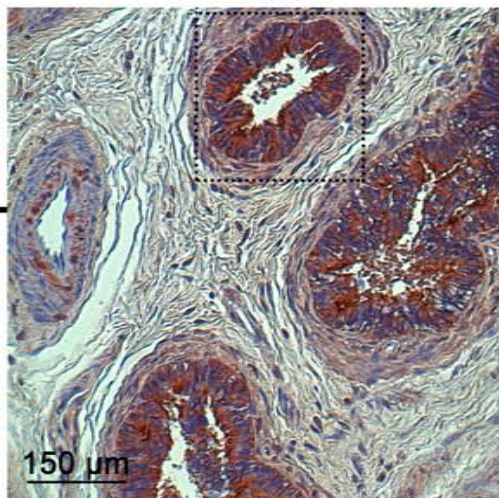
A**PC1-PND7****PC1-PND40****B****Ac-Tub****PC2****Merge****Ac-Tub****PC2****Merge**



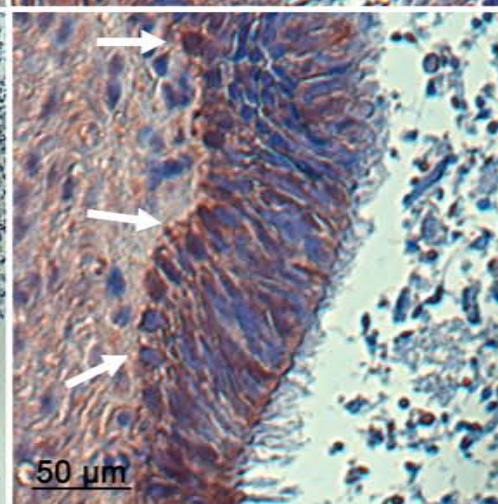
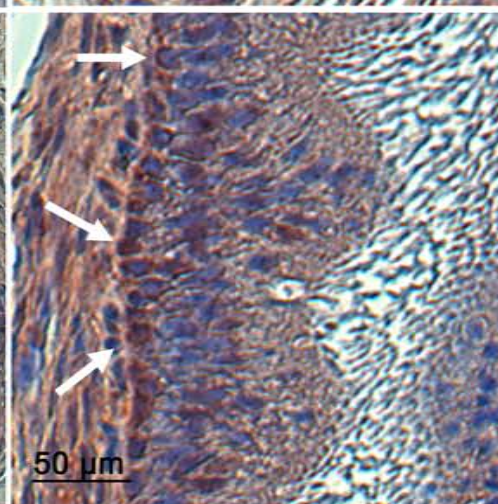
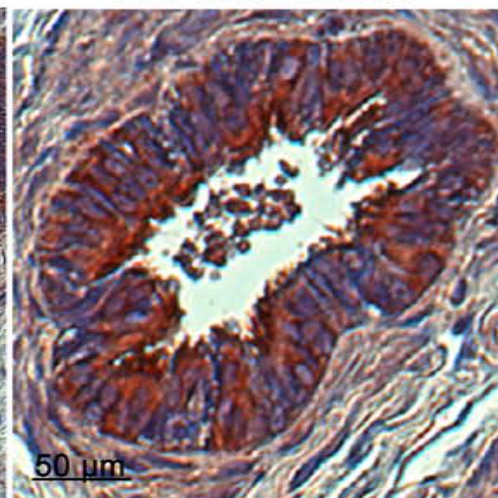
Human epididymis



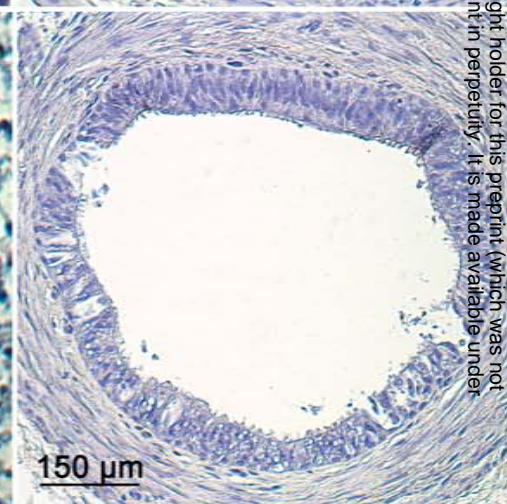
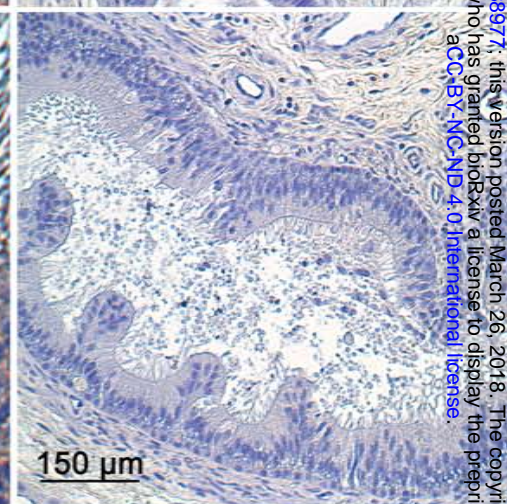
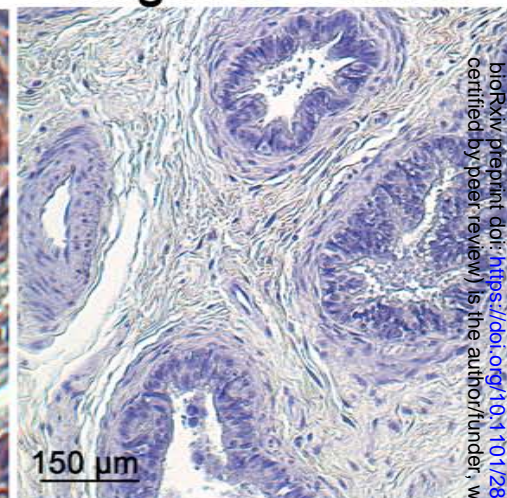
Arl13b



Arl13b-Inset



Negative control



bioRxiv preprint doi: <https://doi.org/10.1101/288977>; this version posted March 26, 2018. The copyright holder for this preprint (which was not certified by peer review) is the author/funder, who has granted bioRxiv a license to display the preprint in perpetuity. It is made available under aCC-BY-NC-ND 4.0 International license.

